LOCALLY PATTERNED CARBON NANOTUBES FOR IN SITU SENSING OF DEFORMATION AND DAMAGE IN COMPOSITE MATERIALS

by

Rossiny Beaucejour

A thesis submitted to the Faculty of the University of Delaware in partial fulfillment of the requirements for the degree of Bachelor in Mechanical Engineering with Distinction

Spring 2014

LOCALLY PATTERNED CARBON NANOTUBES FOR IN SITU SENSING OF DEFORMATION AND DAMAGE IN COMPOSITE MATERIALS

by

Rossiny Beaucejour

Approved: _____
Erik Thostenson, Ph.D.
Professor in charge of thesis on behalf of the Advisory Committee

Approved: _____
James Glancey, Ph.D.
Committee member from the Department of Mechanical Engineering

Approved: _____
Matthew DeCamp, Ph.D.
Committee member from the Board of Senior Thesis Readers

Approved: _____
Michelle Provost-Craig, Ph.D.
Chair of the University Committee on Student and Faculty Honors

ACKNOWLEDGMENTS

I would like to thank the Ronald E. McNair Scholars program, University of Delaware Office of Undergraduate Research and Experiential Leanring, and the National Science Foundation (Grant No. 1138182, Dr. Mary Poats, Program Director) for funding this project. Special thanks go out to the University of Delaware Center for Composite Materials and the University of Delaware Mechanical Engineering Department at Spencer 311 Laboratory.

Thank you to Zach Melrose for providing training and starting the project. Thank you to Gerard Gallo for the assistance on the Instron. Special Thanks to Dr. Erik Thostenson for being a wonderful advisor and guiding this project to success.

TABLE OF CONTENTS

LIST OF TABLES

LIST OF FIGURES

ABSTRACT

Carbon nanotubes (CNT) possesses many properties that deem the material to be multi-functional and capable of being used for various applications. Carbon nanotubes can improve the overall strength, modulus, fatigue life, and thermal properties of polymers and composites. Percolating conductive networks of carbon nanotubes are capable of detecting deformation and damage in materials. Nanotube composites possess strain-dependent electrical properties that enable carbon nanotube deposited ink sensors to be used in health monitoring systems.

Screen printing is a scalable way to incorporate carbon nanotube-based inks into composites for patterned sensors. This research focuses on formulating carbon nanotube inks for creating patterned sensors and evaluating their sensing response in composites. The properties of the ink are first characterized and used to produce the patterned sensors. The addition of cellulose, Polyox^{TM}, and polyvinylpyrrolidone (PVP) provide the desired rheology to enhance print quality onto glass fibers. Concentration and performance evaluations permit the creation of tailorable inks depending on different precursor solutions and application. To understand the performance of the carbon nanotube sensors composites are mechanically tested under quasi-static and cyclic loading conditions. Acoustic emission and edge replication is used to confirm the ability of the nanotube printed sensors to be used in structural health monitoring systems and monitor crack, strain, and permanent deformation in composite materials.

Chapter 1

INTRODUCTION

1.1 Composite Materials and Damage Sensing

The use of composite materials continues to increase in every industry. Due to the complex nature of fracture in composite materials the initiation and propagation of damage is difficult to detect. Current approaches for analyzing damage include a variety of non-destructive evaluation (NDE) [5, 16] and structural health monitoring (SHM) [6] techniques. NDE techniques are generally offline processes that can be very time intensive and SHM involves using a continuous, real time, robust network of sensors to evaluate damage. *In situ* sensing with carbon nanotubes (CNT) provides an opportunity form electrically conductive nerve-like networks in the polymer matrix of composites to examine detect damage. This approach can potentially be utilized as either a NDE or SHM technique.

1.2 Carbon Nanotube Properties

The discovery of carbon nanotubes a few decades ago captured the attention of numerous researchers and industry. The carbon nanotube electrical characteristics, microscopic size, and other features enable them to act as a multifunctional reinforcement. Pandey and Thostenson [10] recently reviewed the multifunctionality of polymer nanocomposites based on carbon nanotubes. For use as sensors, the nanotube-nanotube electrical tunneling gap changes in response to overall strain and

result in a bulk change in electrical resistance that is higher than expected based on mechanical deformation. Carbon nanotubes also can increase the stiffness and strength of the composites. While the conductive nature of nanotubes allows the material's resistance to be measured, its mechanical properties increase the overall strength of the host specimen.

Many methods exist to integrate carbon nanotubes into composites. This research focuses on using screen-printing to selectively pattern carbon nanotubes directly onto fibers. To produce carbon nanotube inks, various fillers were added to enhance the print quality. Characterizing the carbon nanotube dispersions with the right amount of additives will enable the development of nanotube-based inks for screen printed with a high degree of repeatability and tailored electrical conductivity. Screen printing provides a scalable to integrate nanotubes onto composite fabric. During testing, the changing in resistance over resistance was used as a gauge factor to represent strain. The percentage change in resistance, $(\Delta R/R)*100$, was correlated to damage to evaluate the performance of the sensors.

1.3 **Carbon Nanotubes Potential Sensing Applications**

Nanotubes have many applications from nanoelectronics, nanocomposites, characterizing material properties, and much more [10]. The technique of detecting deficiencies has evolved and taken the forefront for most safety inspections. In aircraft inspections, it takes hours to approve the vehicle for operation. Damage sensing and the development of other technologies decreased the amount of time it takes to complete these audits. With the implementation of carbon nanotubes, a new era of damage sensing will arise with the ability to print nanotubes onto composites. By

exploiting the chemical's electrical properties, deformation can be measured by comparing an increase of electrical resistance to material failure.

Applying localized and patterned carbon nanotube sensors printed over the fuselage may significantly shorten the duration of inspections. Localized damage will interact with the nerve-like system, which can determine the location and type of damage. The CNT sensors would be used to analyze stress, failure mechanisms, and microcscle damage within a composite. Several properties can be explored by comparing the resistance to other desired functions.

Chapter 2

LITERATURE REVIEW

2.1 Physical and Electrical Properties of Carbon Nanotubes

Carbon nanotubes possess many characteristics, providing motivation for researchers to continuously discover and exploit their physical and electrical properties. The various properties allow carbon nanotubes to be multi-functional and able to be used for many applications. Researchers have reported that carbon nanotubes improve the overall strength, modulus, fatigue life, and thermo-mechanical properties of polymers and composites [15, 17]. In Figure 2.1, Thostenson *et al.*[15], shows a schematic of the dispersion of nanotubes into traditional fiber composites. Smaller than most fibers, carbon nanotubes are able to penetrate the fiber bundles and create electrically percolating networks. Nanotubes are three orders of magnitude smaller than most fibers and its high aspect ratio makes it a great candidate for the formation of electrical networks [15]. The carbon nanotubes are able to infiltrate gaps between the fibers and can wrap around individual fibers.

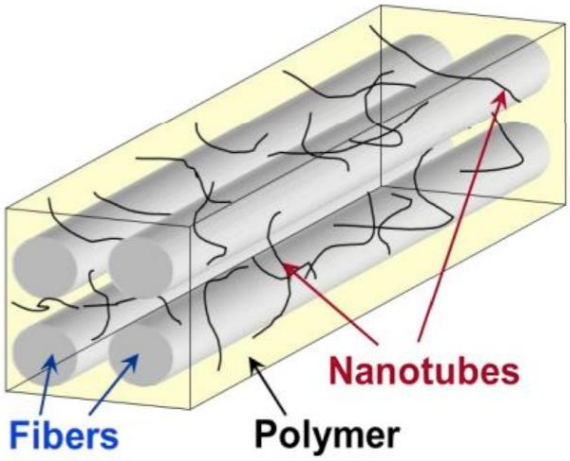

Figure 2.1 Carbon nanotubes impregnated into the polymer can penetrate the matrix of the fibers [16].

The most unique features of nanotubes are their ability to conduct electricity, opening doors for the fabrication of sensors. Small volumes of nanotubes form an electrically percolating network allowing current to flow in the insulating polymer [4, 10]. Nanotube composites have strain-dependent electrical properties that enable the creation of sensors to be used as potential health monitoring systems. Pandey *et al.* [10] reports that nanotubes are initially in an agglomerated state and in order to establish nanotubes as percolating electrical networks, the agglomerates must be separated. The untangled state not only improves the electrical conductivity but also increases the stiffness of the polymer matrix [16]. Once electrical networks are established, nanotubes can be used as piezoresistive sensors for many applications. Piezoresistive sensors utilize the electrical resistance change of a material to measure changes in pressure, strain, force, or acceleration. As cracks propagate in fiber composites the materials experience a permanent change in resistance because the nerve-like carbon nanotube network is severed, enabling the measurement *in situ*. In

the elastic regime the resistance changes due to the nanotube-nanotube contact resistance that correlates to the amount of strain being applied. If no damage occurs, this resistance change is reversible. In this research the piezoresistive responses in nanotube printed sensors are thus used to detect cracks and strain. Understanding resistance measurement of damaging in materials provide insight on how it fails and further research can be done to reinforce the materials or prevent failure form accruing in the first place.

2.2 **Chemical and Physical Properties of CNT Ink Additives**

Small percentages of nanotubes increase the viscosity of water-based solutions but do not have the desired rheology for screen-printing. Successful printing requires supplemental additives like cellulose, polyethylene oxide (Polyox) and polyvinylpyrrolidone (PVP) in solution with nanotubes. Cellulose has thickening and binding capabilities that drastically increases the viscosity when prepared with liquid solutions and can be found as a common additive in cleaning products, personal care, sealants, caulks, and other coatings. Cellulose is a very desirable supplement for nanotube dispersions because the material is economical, environmentally friendly, and renewable.

Cellulose is polysaccharide made of thousands of D-glucose units. The intermolecular hydrogen bonding makes the material very bulky and insoluble in water. Carbon nanotubes and other additives can interfere with the hydroxyl groups decreasing the strength of the polymer. Bonding between CNT and cellulose result in co-solubility, which makes cellulose a great candidate for carbon Nanotube dispersion. Without cellulose, nanotubes precipitate when dispersed in water. Cellulose suspends

individual carbon nanotube strands in solution allowing for a more complete dispersion [1, 17].

Cellulose is the preferred addition for water-based solutions because it's large range of stability under varying pH. Adsul *et al.* [1] indicate that water-based solutions require a pH between 6 and 10 in order for cellulose and nanotubes to be well dispersed. When the pH of the water is out of this range the nanotubes and cellulose precipitate from solution. In order to be useful for applications, carbon nanotube dispersions must be stable and with no agglomerates.

PVP acts as a stabilizer and dispersant and can be found in toothpaste, hair products, creams, and lotions. PVP is a surfactant, and contains elongated chemical chains with each pyrrolidone connecting to a polyethylene chain that wrap around the carbon nanotubes [9]. The addition of PVP to cellulose and carbon nanotube dispersions lowers the surface tension while keeping the solution stable. PVP also reduces the sedimentation velocity but does not change the overall viscosity of the solution [11]. PVP plays an important role of stabilizing the ink solutions used in this research.

Polyox functions as a lubricant, binder, and film former when dissolved. Polyox is commonly used in fillers, powders, ceramics and pigment [7]. The addition of Polyox ensures homogeneous dispersions of carbon nanotubes and holds the nanotubes in place, guaranteeing electrical conductivity for the percolating networks. Effective dispersion of all elements is critical for carbon nanotube-based inks to prevent clusters from forming, impeding effective nanotube electrical connections.

2.3 **Pre-Printing Processes**

Screen printing techniques have been utilized in the graphics industry for quite some time. Recently, researchers have applied printing techniques to deposit carbon nanotubes for the manufacturing of piezoelectric sensors in the medical filed and for engineering applications [13, 14, 18]. Because screen-printing is inexpensive, safe, and a quick method for mass-producing patterns, it holds potential as an efficient method for the fabrication of various types of electro sensors. The screen-printing process has been used for TV applications and other biotechnical sensors [12].

Prior to the successful fabrication of sensors, effective processing must take place to ensure the ink solutions are well dispersed, stabilized, and free from agglomerates. Pandey and Thostenson [10] report that the processing conditions including, pressure, temperature, nanotube position and mixing duration will modify the electrical properties of composites. All aspects of the processing conditions must be analyzed to achieve the desired results. Depending of the composition of the ink, the pH must also be adjusted in order to keep dispersions stable. During fabrication of insulin sensors, Rafiee and co-workers [12] modified the pH using boric acid and sulfuric acid. Kroger *et al.* [8] used methanol and phosphate combinations to neutralize and modify the screen-printed electrode inks. Piezoresistive screen inks are only effective when used at a neutralized state. When the pH is out of range, additives and carbon nanotubes will not be completely disperse into the solution. Incomplete mixtures interfere with the electrical properties of the carbon nanotube network.

The disruption of nanotube networks is caused by nanotubes clumping together, which decreases their effective aspect ratio (length/diameter). These agglomerates reduce the number of nanotubes involved in the percolating network,

which increases the overall resistivity. Thostenson and Chou [16] used the three-roll mill as a standard for removing agglomerations from solutions. The technique results in larger nanotube aspect ratio as opposed to other techniques due to the intense shear mixing as the gap setting is lowered. With each pass, the nanotubes are stretched out as they pass through the gaps of the mill and are gradually untangled [4, 15]. If the roller gaps become too small, there exists a potential for the nanotube to be degraded, reducing their participation in the percolating network.

Ultrasonic techniques provide an alternative for dispersing nanotubes into solution. Three-roll milling requires mixtures to have a high enough surface tension in order to prevent the material from dripping off the rollers. In low viscosity solutions, sonication is often method for dispersion. Adsul and co-workers [1] used sonication techniques to combine carbon nanotubes and cellulose in distilled water. Although a time intensive process, sonication provided a safe way to mix nanotubes without material degradation. All inks are prepared with distilled or multiple rinsed distilled water to prevent contaminates from disrupting the intermolecular bonding and producing unfavorable solutions. Using ultra purified and distilled water keeps pH consistent during the sonication process.

2.4 **Printing and Post Processing**

Screen-printing can be executed using traditional hand printing methods or using machines if sensors require small, accurate prints. Kroger *et al.* [8] used DEK248 (semi- automatic printer system, Asflex S.A. Int., Spain) to deposit carbon electrodes for creating biosensors. Sanchez *et al*. [13] also used the DEK248 machine and applied the double-sweep technique for printing. Depending on the size of the

sensor required, a machine or traditional screen-printing press can be used to create patterned prints of nanotubes onto sensors. The double stroke method, where the blade is passed twice over the screen, is standard in ensuring all voids all filled. Yukui *et al*. [18] utilized the method of screen-printing for producing field emission displays devices.

An understanding of the printed sensor morphology and resulting electrical properties is essential to assessing its ability to sense deformation and damage. The nanotubes must form a continuous percolating network when printed, as local variations in the morphology may alter the global sensing response. Sensors must possess electrical capabilities and sufficient print quality to be considered for operation. It is essential to have knowledge of how processing affects the print quality and resulting electrical response. In this work microscopy is used to analyze the wicking tendencies of the ink and the relationship between the formations of nanotube networks.

Inks generally contain a significant amount of solvents, such as water. It is necessary drive-off the solvent so that the inks form a solid film in order retains the desired print pattern. Sanchez *et al.* [13] used thermo-gravimetric analysis to probe for moisture and impurities and then cured parts with a furnace at 120°C and again to 1000°C. Afterwards, the samples were analyzed using atomic force microscopy. Kroger *et al.* [8] cured samples at 125°C for 2 hours. Shi *et al.* [14] removed moisture and organic binders at 350°C but also reported using UV laser lights to radiated sample. Various methods, temperature settings, convention and radiation techniques exist to remove impurities from inks. In order for successful use of electro sensors in a composite, all of the moisture must be removed to retain percolating network

connections. The solid content of inks must contain sufficient volume fraction of carbon nanotubes in order to create conducting pathways.

2.5 **Interpretation of Electrical Responses**

Nanotube-based sensors have been found useful in mass, humidity, and strain sensors and electromagnetic actuators [16]. A majority of the sensors function on the ability of the piezoelectric property of CNT to change resistance as stress is applied. The changes in electrical properties of the carbon nanotube network due to deformation and the formation of micro-scale damage can provide researchers with feedback structural health of the system. The ability to correlate changes in resistivity with the propagation of cracks provides a potential opportunity for quantitative determination of the damage state. Gao *et al.* [3] reported using change in resistance per unit length and change in resistance per original resistance to analyze the health of composites as various loads are applied. Thostenson *et al.* [l5] also used to change in resistance per unit length to correlate the damage to the crack density which is the amount of cracks per unit length of the sample. Both experiments were successful in associating change in resistance to deformation in the composites. As the loading conditions were modified, sensors adequately detected the formation of cracks in proportion to the variations in resistance. The change in resistance per length corresponds to the accumulation of damage due to transverse microcracks in cross-ply specimens [3]. The damage accumulates progressively until the entire specimen fails [16].

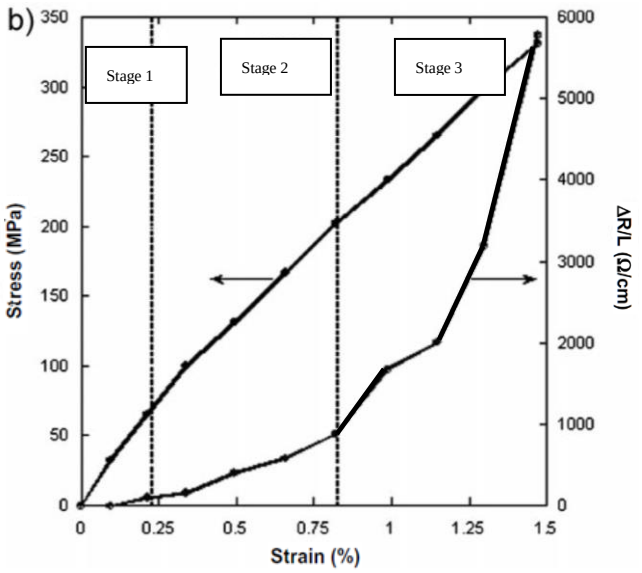

Figure 2.2 Stages of damage in a fiber composite with [90/90$_2$/0] orientation sensed by carbon nanotubes is displayed in the image above. Stage 1 is crack imitation, 2, transverse microcracking, and 3, cracking and delamination [3].

Understanding the feedback of materials in different loading conditions and orientations will reveal information about the magnitude and type of failure mechanisms it experiences. In Figure 2.2, three stages of failure are presented to model the material cracking and failure and the carbon nanotube resistance response. In the first stage, called crack initiation, where micro-scale damage is initiated due to fiber-matrix interface de-bonding in the transverse plies while unidirectional plies remain elastic. In stage two, transverse microcracking, the material is deformed as the 90-° initial damage coalesces to form transverse micro-cracks. The shear-lag theory causes the cracks to saturate at a uniform spacing along the length of the 90° plies.

During stage three, delamination, the slope of the resistance curve increases dramatically, the strength decreases, and the layers begin to separate [3]. Various modes of failure are determined form analyzing the resistance curves in the sensors. All three stages experience distinct electrical responses, which can inform an experienced researcher on the state of damage.

2.6 **Advanced Application and Damage Confirmation**

In real-world applications, material stresses do not always occur under tensile loads. Under out-of-plane and compressive loads, nanotube sensors are also responsive. Progressively increasing cyclic loading tests provide an advanced testing method to understand more about material failure. Under cyclic testing conditions, Gao *et al.* demonstrated the concept of damaged resistance change (DRC). As the specimen experiences crack re-opening, DRC takes into account the accumulation of the permanent change in resistance with each load cycle [4]. When the load is released in latter cycles, the resistance does return to its original state revealing that some of the percolating network is reconnected by crack closure [15]. Such responses demonstrate the capability of these sensors to be used to detect micro-cracking, delamination, and permanent deformation. Resistance measurements in the sensors follow the load and unload series of the fatigue cycles very well.

Acoustic emission (AE) is an accepted method of testing for damages in materials and has been utilized to validate the carbon nanotube-based sensing response. AE uses sensors record the energy released by the stress waves formed when a material cracks under certain loads. AE is able to measure new damage and provides and safe and non-destructive technique of measuring damage. AE sensors are used in

civil engineering, mechanical structures, manufacturing, and in advanced materials [2, 5].

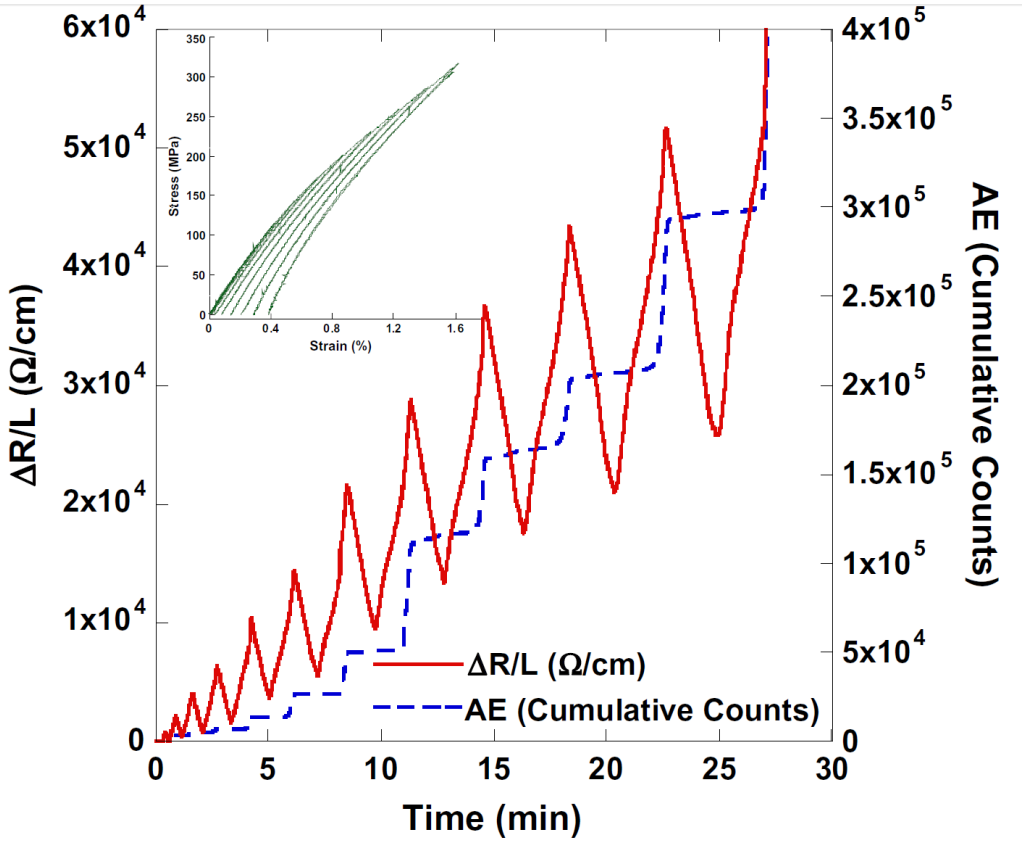

Figure 2.3 Acoustic emissions and piezoresistive response of the composite is displayed in the electrical data above [5].

In Figure 2.3, AE hits match the drastic changes in resistance of nanotube sensors, providing insight on what occurs at the peaks in resistance measurements. Since acoustic emission sensors are only able to detect the onset of new damage, it is a great tool for confirming spikes in resistance and correlating to new fiber breakage. Although AE provides evidence to prove that nanotube sensors are accurate in the

reporting damage, it cannot be the lone device in depicting failure in material. AE signals cannot differentiate the various modes of failure and extra noise from Instron grips or reverberated sound waves. Thus, the results are primarily qualitative.

Chapter 3

METHODOLOGY AND EXPERIMENTAL METHODS

3.1 Characterization and Processing of Carbon Nanotube Dispersions for Damage Sensing

The development of the carbon nanotube inks is an iterative process separated into four stages. The preliminary stage includes the characterization and processing of the carbon nanotubes with other additives and fillers to produce the desired printing rheology as represented in overall research approach shown in Figure 3.1. Various weight percentages of cellulose (Cellosize QP 52000, Dow), polyethylene oxide (Polyox) and polyvinylpyrrolidone (PVP K-90, Ashland Inc) were added to establish the right composition after the nanotubes are dispersed. In this experiment, an analytical balance is used to weigh out carbon nanotubes and additives. A standard top loading balance of a gram was used to measure resin, epoxies and other chemicals. The naming scheme established for the different solutions follows the formula N-A_B_C. The letter N signifies the percentage of nanotubes dispersed in solution. The letter A represents Cellulose, B for Polyox and C for PVP. The solutions are labeled to differentiate every batch.

The process begins by filling a bottle with 40 grams of triple rinsed distilled (TRD) water. TRD is ultra-purified water prepared with filtering techniques and boiling and condensing water to remove contaminates. Original solutions were developed using sonication, thinky mixer, hand mixing, and mixing paddle. The Vankel 7000 U shaped paddle produced the best homogeneous solution. The U-Paddle

was used to amalgamate Polyox, PVP and cellulose, respectively. Cellulose is the main thickener for the solution so is must be added last since it creates irreversible changes to the viscosity. Once cellulose is dispersed in solution, it is difficult for other additives to dissolve adequately in the ink.

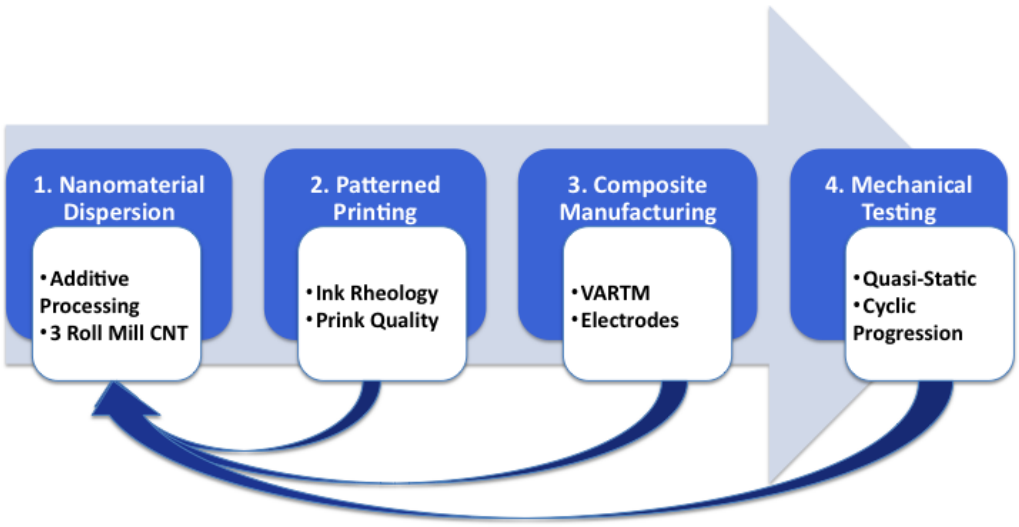

Figure 3.1 The manufacturing approach for patterned sensors is an iterative process with 4 stages.

Cellulose is the main thickener for the solution so is must be added last since it creates irreversible changes to the viscosity. Once Cellulose In solution, it is difficult for other additives to dissolve in the ink.

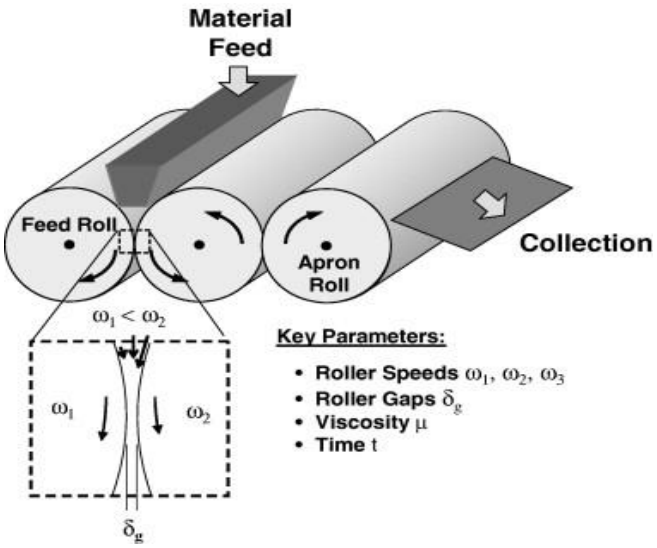

Figure 3.2 Three-roll mill calendering technique is used to process CNT and polymer [16].

Table 3.1 Three- roll mill calendering sequence begins with a large to small gap setting.

Gap Setting (Nanometers	*Number of Passes*
20	5
15	3
10	3
5	10

Polyox must be integrated very carefully because it has a tendency to stick to itself and create agglomerates that cannot be separated. The mixing process must be restarted if Polyox does not fully dissolve. The solution continues to mix at 100 RPM with the U-paddle for one hour. Carbon nanotube powder from Hanwha Nanotech is then added to the solution. The person executing the tasks must use a fume hood wear

a mask to prevent from inhaling the nano-material. The solution is then cycled through a calendering process, shown in Figure 3.2, using a three-roll mill (EXAKT 80E, EXAKT Technologies, Inc.) to disperse and detangle the nanotubes into the ink. Nanotubes are highly entangled in their bulk form and extra processing is required to separate the nanotubes and disperse them in order to form a conductive percolating network of nanotubes in the solution. The final inks were assessed by measuring the pH with a pH meter, taking digital microscopic images using DinoCapture, and using a rheometer to measure the viscosity.

3.2 **Screen Printing Technique**

Stage two consists of applying basic screen-printing tools and techniques to print the ink onto reinforcing fabric. It based on previous experience is important that the conductivity of the as-printed nanotube sensors have a resistance in the kΩ range or below in order to have enough sensitivity to sense damage. If the print quality is not sufficient, the experiment will be reverted back to stage one, as indicated in Figure 3.1. Before the initiation of the printing process, the material is hand mixed until the composition is uniform. If the batch is small, a Thinky planetary mixer is used to mix the ink for one minute to ensure dispersion.

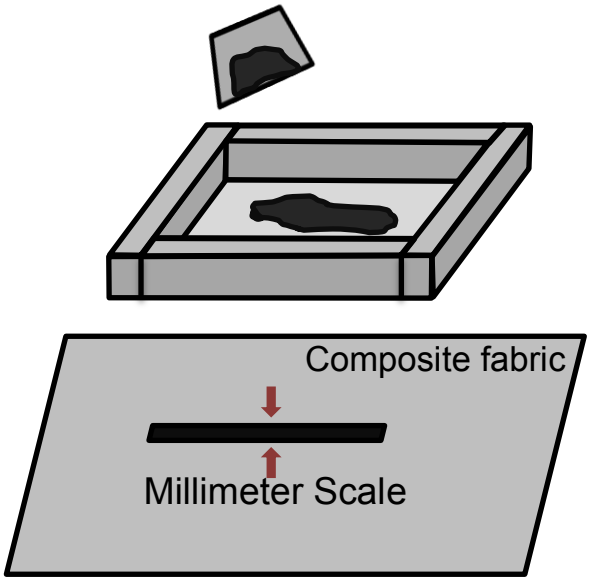

Figure 3.3 Traditional screen-printing technique used to deposit CNT.

The traditional screen-printing technique displayed in Figure 3.3 is used to deposit the nanotubes ink onto the glass fiber. One forward and backwards sweep is standard from one print. Too much sweeping induces wicking in the fabric and only one pass generally does not yield a high-quality, uniform print. The screen print board consists of a mesh that has been coated with a resin and then photo degraded under a mask to create desired patterns. For each specimen, ink solutions of 0.0254 to .1524 m (1 to 6 inches) in length are printed onto a 0.177 x 0.17.7 m (7x7 inch) portion of unidirectional glass fabric. The prints are then cured at 90°C for 240 minutes to remove all impurities and moisture. This step is necessary in order for the ink to be conductive and adhere to the fabric surface. By removing the moisture, the conductive network cannot shift and nanotube pattern is locked in place. The electrode regions

were coated with flash dry silver paint (SPI Supplies Division of Structure Probe International) to allow good electrical contact and not require excessive sanding of the sensor after composite processing. A digital multi-meter was used to measure the resistance to ensure that the sensor in the kΩ for resistance.

3.3 **Manufacturing: VARTM, Electrodes, and End Tabs**

Stage three involves embedding the nanotube sensing fabric with other layers of fabric to form a composite. Following Gao and co-workers [2] vacuum-assisted resin transfer molding (VARTM) was used to impregnate the different layers together with resin. VARTM is achieved with a ratio of 1 to .264 of Epon Resin 862 and Epikure W curing agent. Both chemicals were purchased from the Miller-Stephenson Chemical Company (Resolution Performance Products). Before infusion the resin must be degassed to remove any bubbles. Air or other volatiles will cause voids in the part once it has cured, affecting performance of the composite. The resin is degassed twice at 60°C for ten minutes with a vacuum oven while the fabric is also preheated to 60°C. The elevated temperature reduces the resin viscosity and subsequently increases the rate at which the resin infiltrates the glass fiber.

Multiple orientations exist to configure the fabric for VARTM. In this experiment, we use five zero degree orientations to established unidirectional laminates and three layers of 90°orientations between two zero degree laminates to establish a cross-ply configuration. The arrangement of the plies will show different damage mechanisms, generating diverse modes of failure for each composite. Zero degree plies are stronger and stiffer than the 90° plies and carry the most of the applied load. The part is cured at 130°C for six hours in a convention oven with a vacuum attached during the entire process. The pump and vacuum ensure there are no air

bubbles in the part and keeps the layers of fabric compressed while infusing the resin all the way through the part. End tabs are then attached to the composite once the VARTM process is complete. The composite and end tabs are sand blasted at bonding sites to enhance adhesion. Hysol (Part 1.0A and .22 B) from Henkel Corporation is used to bond the composite and end tab. The bonded parts are then cured at 90°C for 30 minutes.

The sensors are wet sanded to remove the layer of resin on top of the ink to reach the silver paint. Over sanding can cause the sensor to be destroyed. The reaching the silver paint confirmed by using a digital multi-meter to measure the resistance, where a reading in the MΩ range indicates more needs to be eradicated to penetrate the conductive layer. An off scale reading indicates that the sensor has either been damaged or there is still a layer of resin on top of the sensor. The composite is then machined ten tensile specimens using a wet saw with a blade with of 1.78 mm (0.7 inches). Afterwards, electrodes are attached for two wires sensing using electrically conductive silver epoxy (.5A and .5 B) from Innovative Bonding Solutions ETC. Conductive epoxy is required to prevent the adhesive from separating the electrode from the percolating CNT network. The part is then cured at 90°C for one hour. Once the process is complete the resistance is measured to confirm the sensor is viable. Resistive strain gages were bonded to the specimen to measure strain.

3.4 **Testing: Resistance, Stress and Strain, Crack and Damaging Sensing**

The final stage of the process consists of testing the specimen to assess the nanotube sensors ability to sense damage sensors. Following Lim *et al.* [4] the specimen sensor was attached to a digital multi-meter, and acoustic emission sensor

(Figure 3.4) to simultaneously measure electrical resistance while the material is deformed to failure.

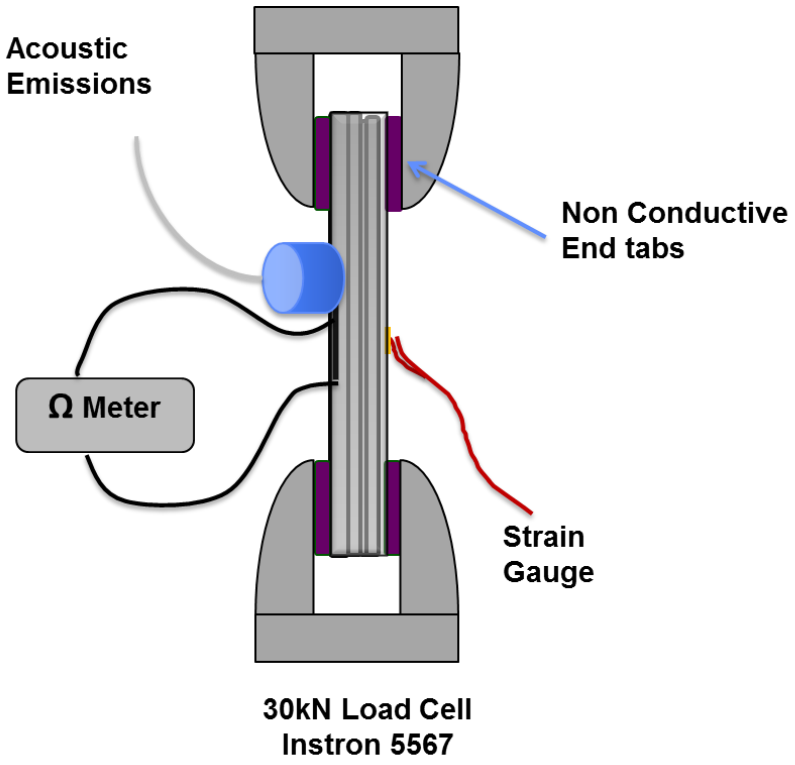

Figure 3.4 Mechanical testing apparatus is used to perform monotonic and progressively increasing cyclic quasi-static tensile tests.

For specimens that fail at over 1,000 pounds of force, a 5,000 lb. load cell is used with screw driven load frame (Instron 5567 or Instron 5565/5567, 5/30kN load cell for nanocomposite tensile bar/patterned composite) A NI PXI 4300 analog card is used to acquire data from the load frame. A Labview .vi) is used to compile resistance, strain, and loading data for real-time analysis. A different Instron will be used for materials that fail at less than 1000 lbs. The two electrodes are connected to a digital multi-meter to measure resistance *in situ*. The acoustic sensor is attached using hot melt glue gun to the composite and measures acoustic events during test. Once the equipment is ready for use, two tensile tests are performed on composites without sensors to establish the baseline performance. Data from the tensile test is used to determine the loading steps in the five cyclic loading tests. The resistance is used to monitor damage progression and accumulations of the parts.

Chapter 4

EXPERIMENTAL RESULTS AND DISCUSSION

4.1 Composition of CNT characterized using Micro-Imaging

The increased concentration of carbon nanotubes in the ink solution creates dramatic changes in ink rheology and quality of the printed features.. The print quality was evaluated after the deposition on the ink onto the fabric. High performance inks were characterized by the how well inks coated the surface of the fabric and filled intra and inter fiber regions in the fabric.. Once the ink is deposited further wicking results in breaking-up of the deposited electrically percolating network. Concentrations of 0.5 wt.% of nanotubes showed the lowest print quality and also had undesirable rheology. The ink was very low in viscosity, which caused immediate wicking after deposition onto the fabric. Figure 4.1 shows an optical micrograph indicating the wicking behavior of the ink along the fibers. There was a 5 mm deviation from the originally printed dimensions along the fiber direction. The picture also shows re-agglomeration of the ink along the fabric. After curing, the no network of nanotubes formed due to the re-agglomeration and an infinite resistance was recorded.

Increasing the concentration of carbon Nanotubes to 2 wt.% solved the issue of wicking but the ink quality remained undesirable. Although the ink no longer showed wicking along the fabric, the high viscosity of the ink resulted in a very thick, non-

uniform coating on the surface.

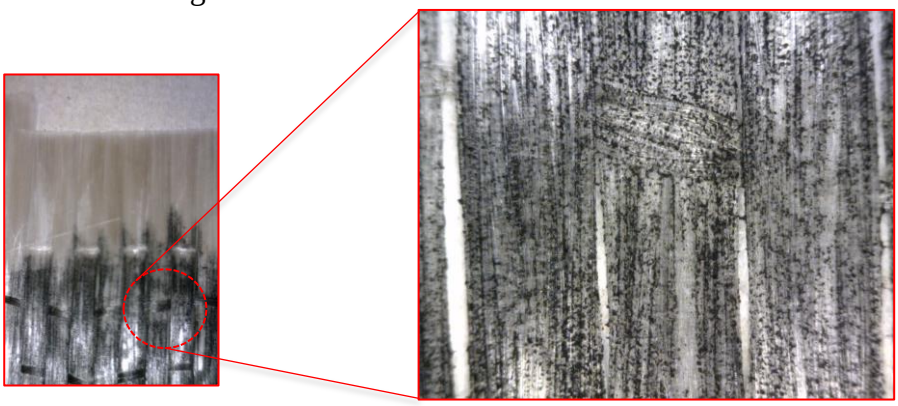

Figure 4.1 Micro-image of .5 % CNT after is printed onto fibers.

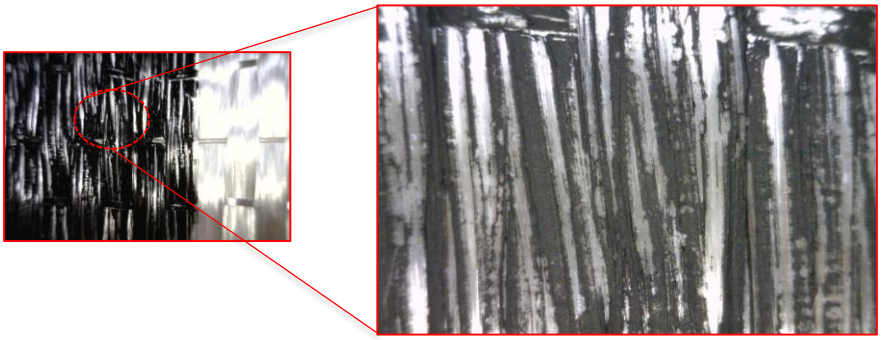

Figure 4.2 Micro-image of 2 % CNT after is printed onto fibers.

As a result, the ink was unable to coat and penetrate the bundles of fibers in the composite. As seen in Figure 4.2 the coating is still very non-uniform. The printed sensor was electrically conductive, but voids in the conductive network decrease the sensor sensitivity. One weight percent of nanotubes in solution was the most effective

composition to enhance print quality. The viscosity of the ink was low enough to allow the ink to penetrate the fiber bundle but high enough to prevent the material from wicking along the fiber, as shown in Figure 4.3. This uniform coating resulted in a highly conductive network formed along the fibers.

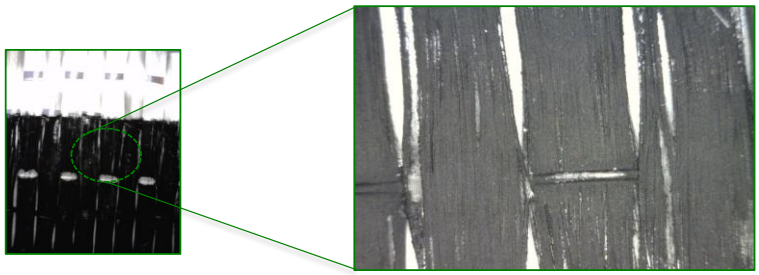

Figure 4.3 Micrograph of 1 % CNT after is printed onto fibers.

4.2 **CNT Interface and Senor Network Characterization Using SEM**

A more complete study of the morphology of the as-deposited percolating networks on the surface of the fiber was accomplished using scanning electron microscopy (SEM). The ability to image materials at the nano-level provides higher resolution and a better understanding of how the nanotubes interact with the fiber surface. In the ideal case with 1 percent carbon nanotubes (1-111), the ink is evenly dispersed and the CNT can clearly be seen and form a connected network. As shown in Figure 4.4, the ink solution flows into the gaps between fibers and creates a continuous coating on the fibers. In Figure 4.5 and 4.6, individual carbon nanotubes can be distinguished from the remaining components of the ink. Although the solution

contains more additives by weight, the nanotubes are still able to establish a percolating conductive network, which is the goal of the experiment.

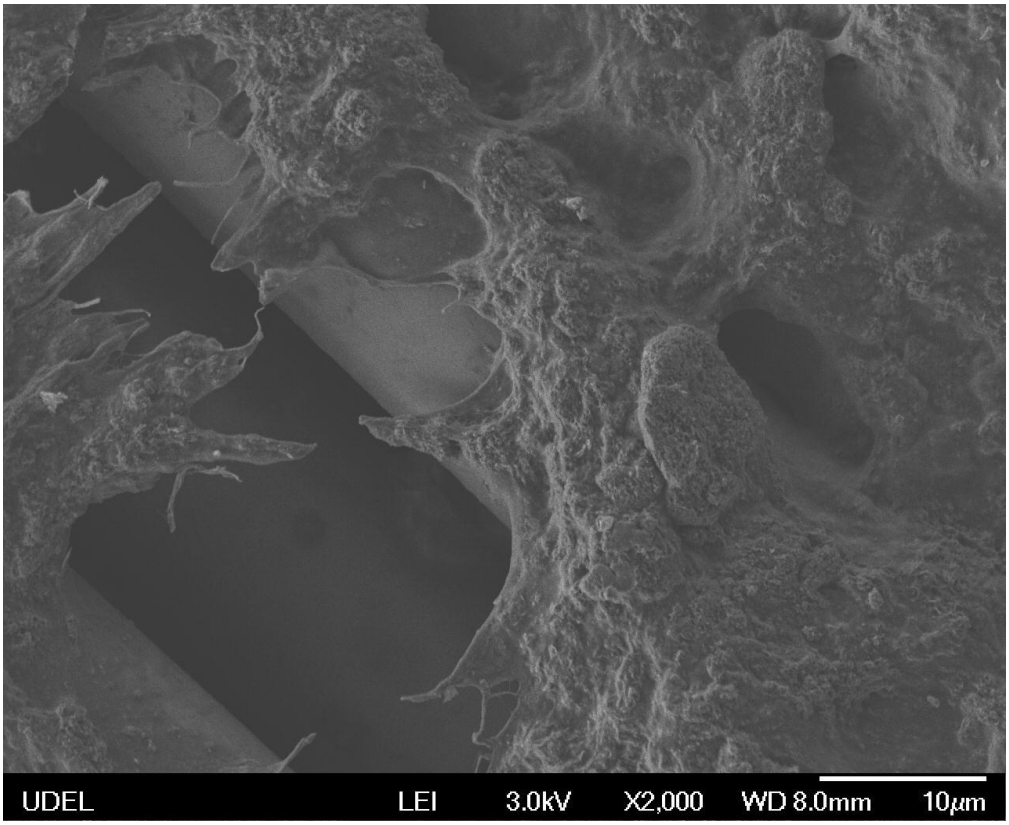

Figure 4.4 SEM image of 1-111 at 2kX after printed onto fibers.

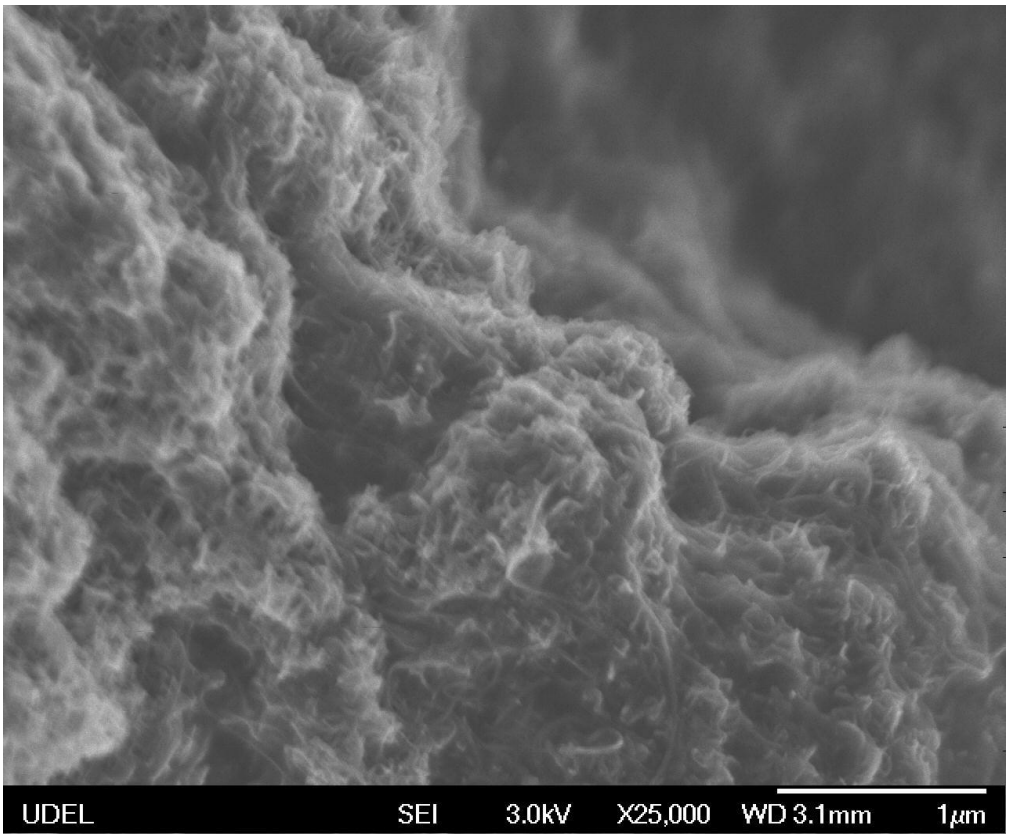

Figure 4.5 SEM image of 1-111 at 25kX after printed onto fibers.

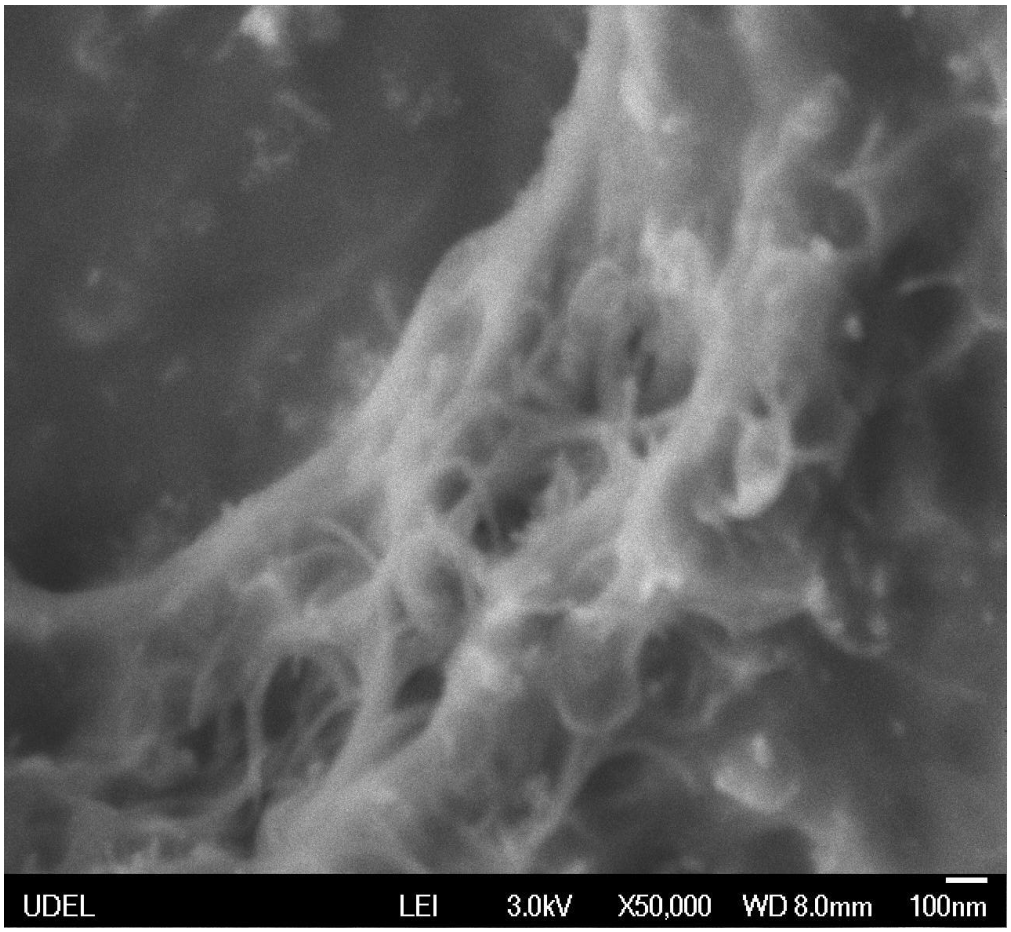

Figure 4.6 SEM image of 1-111 at 50kX after printed onto fibers.

Increasing or decreasing the percentage of nanotubes from the ideal case proved to be infective. at the macro scale, the solution became too viscous for proper deposition onto the fibers. In Figure 4.7, the ink forms agglomerates, which fail to completely coat the interface of each fiber.

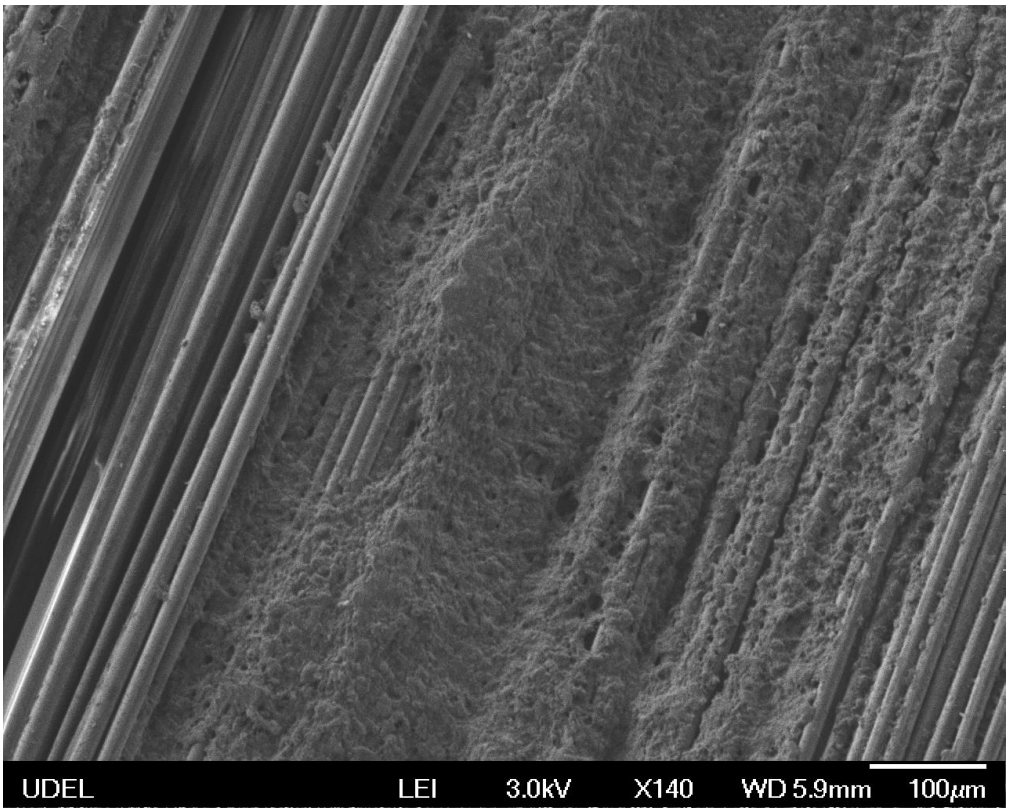

Figure 4.7 SEM image of 2-111 at 140X after printed onto fibers.

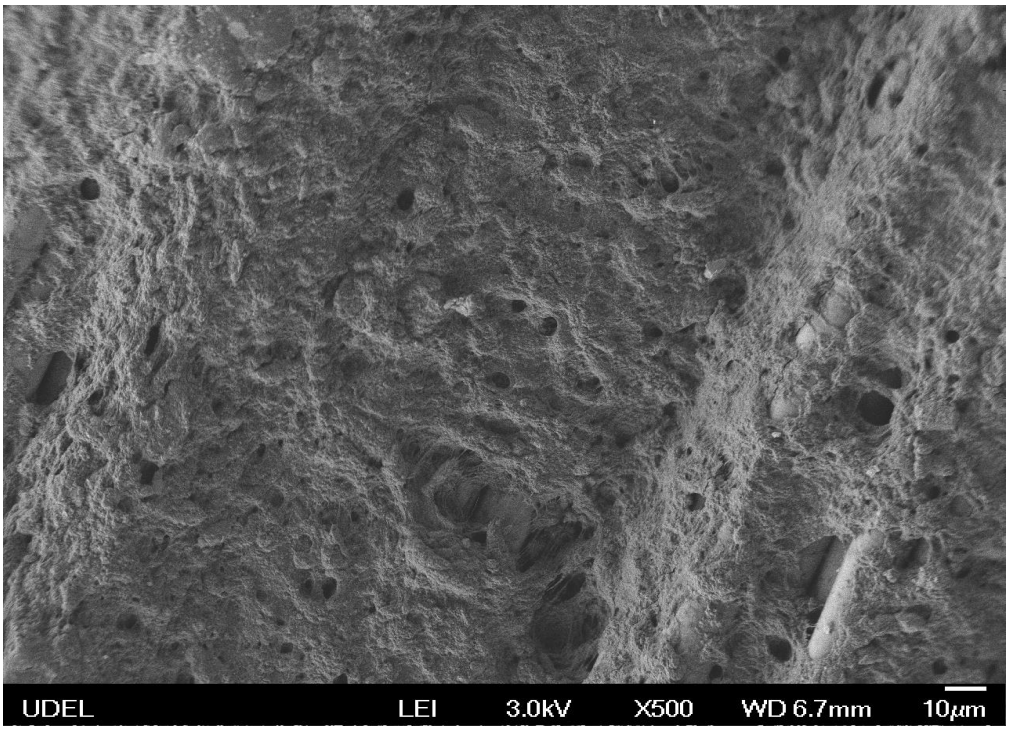

Figure 4.8 SEM image of 2-111 at 500X after printed onto fibers.

Solutions containing 2% nanotubes (2-111) formed a brittle, flaky ink layer. The agglomerates seem to prevent the nanotube networks from connecting although nanotubes can easily be seen. In Figure 4.8 and 4.9 some nanotubes are distinguishable yet it is not clear how well the carbon nanotubes interact.

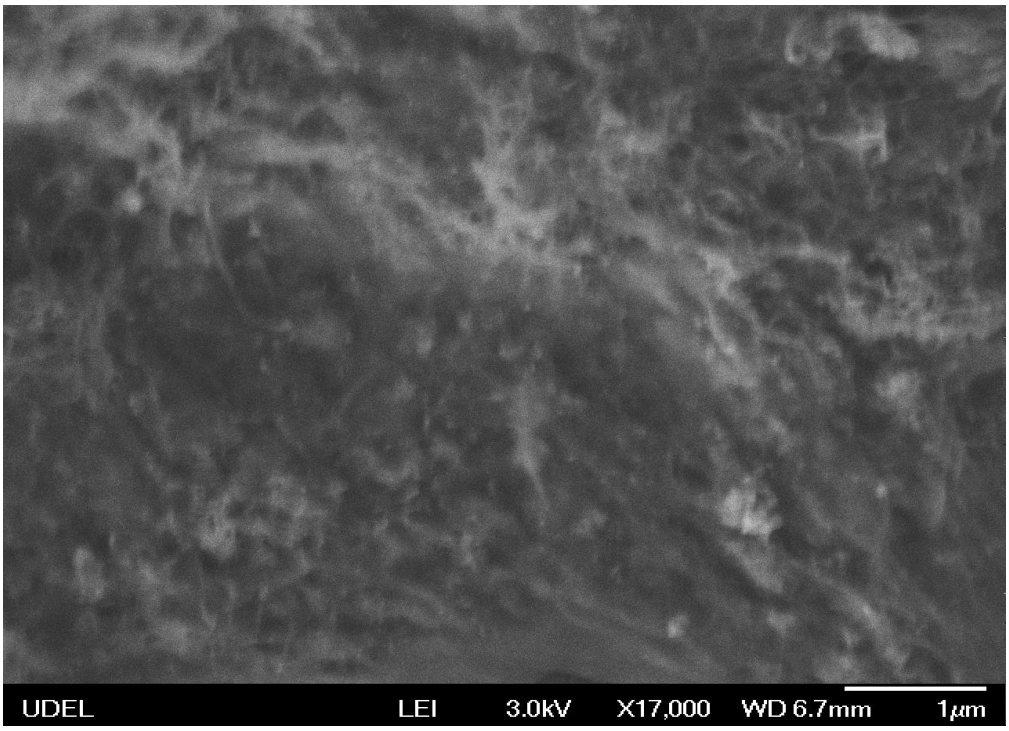

Figure 4.9 SEM image of 2-111 at 17kX after printed onto fibers.

At concentrations of less than 1 percent nanotubes in solution the low viscosity causes the solution to wick along the fiber. The 0.5 wt. % solution (.5-111) also experienced a lot of charging making it hard to capture the images. In SEM, charging occurs when there is a buildup of electrons, which causes abnormal deformation, increases the artifacts, which create noise, and distorts the image contrast. Charging results when specimens are non-conductive. Even after an application of a conductive coating, the images did not provide adequate contrast. This phenomenon further confirms that the 0.5-111 ink was non-conductive

4.3 **Data Manipulation and Processing**

The strain-dependent electrical properties of carbon nanotube composites enable various modes of failure to be identified by analyzing the different resistance responses. The sensor successfully replicated the stress and strain effects induced from the applied load to the composites. When the composite is deformed in compression the tunneling gaps decrease and result in a decrease in specimen resistance. Once the specimens were deformed in tension (Figure 4.10), the resistance increases and the resistance decreases when the load is released, indicating elastic behavior. Once cracks began to form in the composite, the percolating networks of nanotubes were severed, which drastically increased the resistance, indicating material failure.

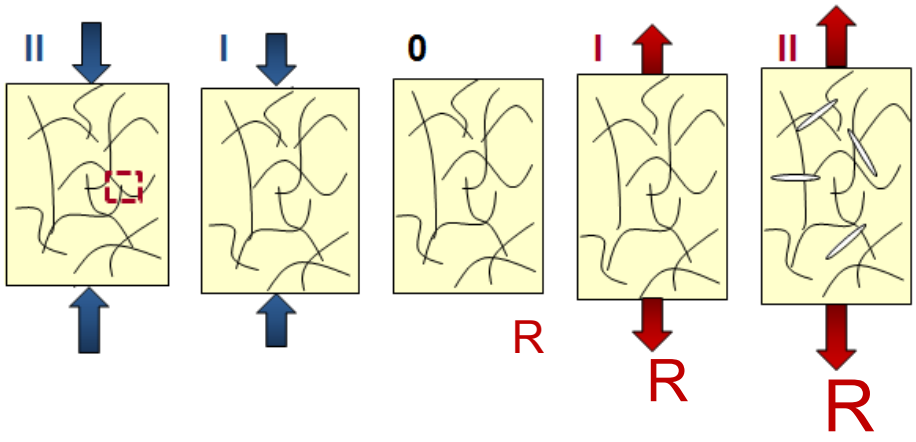

Figure 4.10 Representation of how percolating networks of CNT's behavior under different loading conditions with resistance can change under an applied load.

Stress, strain, acoustic emissions and edge replicates were compare to the resistance to validate the effectiveness of the CNT sensors to screen for damage. For

each data acquisition, the change in resistance over resistance multiplied by 100 (ΔRR/R*100) was used to analyze the percentage of resistance change by the sensor. Converting the load (lbs.) to stress (MPa) correlated to the stresses experienced by the composite to the change in resistance. The resistance curve exhibited a similar slope to the stress curve while also indicating the area where the composite began to experience permanent deformations and cracks. The strain responses also validated the progression of damage in the composites. Resistance and strain followed a similar pattern until the specimen experienced fracture.

Acoustic emissions confirmed the presence of microcracking and areas of high damage with the count total. Expressing acoustic emissions in count total displayed damage accumulation and verified the accuracy of the CNT sensor to detect areas of new damage. Edge replication provided an advanced examination of the cracks and damage accumulation. Jumps in the resistance curves are related to the occurrence of multiple cracks in the edge replicates.

4.4 **Failure Model and Fabric Orientation**

Printed nanotube sensors were patterned onto unidirectional fabric and unidirectional and cross ply composites were fabricated. Unidirectional specimens, in Figure 4.11, are composed of five layers of 0° orientated fabric. Cross-ply laminates consisted of three 90° oriented fabric with one 0°fabric on the top and bottom. Each specimen was loaded to failure under quasi-static monotonic and progressively increasing cyclic loading conditions. In all four cases, the sensors registered distinctive responses. Under all loading conditions, all sensors failed before experiencing a 13%

change in resistance, indicating the effectiveness of the patterned nanotube sensors to be utilized in potential health monitoring systems.

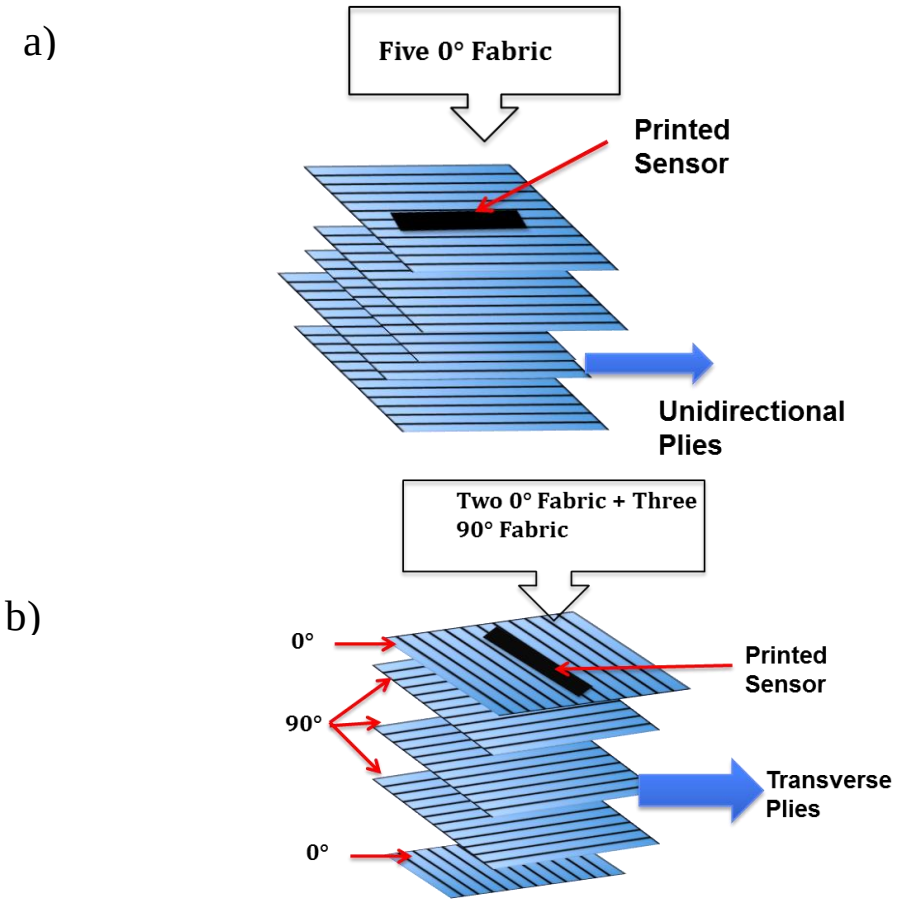

Figure 4.11 Representation of the orientation of 90 degree and 0 degree layers of glass fiber is displayed above. a) Exploded view of unidirectional laminates b) Exploded view of cross ply laminates.

Carbon nanotube sensors have the ability to distinguish the type of damage experienced by the unidirectional and transverse laminates in quasi-static tests. As the load is increased, changes in the slope of the resistance determined the current stage of damage by the composite. Four distinct regions described the damage progression of the composite include crack initiation, transverse-microcracking, unidirectional strain and fracture and delamination. The duration of the four prescribed regions were determined from the orientation of the fabric.

During crack initiation, small cracks begin to form at the fiber-matrix interface and the polymer matrix. In the transverse-microcracking stage, the 90° plies begin to separate and cracks extend towards the interface of the unidirectional plies. After the failure of the transverse plies, the 0° plies carry almost the entire applied load. In this stage the plies have not yet failed but some fibers may experience de-bonding. The last stage, fracture and delamination, the fibers in the unidirectional plies began to fracture or cracks penetrate the layers of the fabric and delamination occurs.

a)

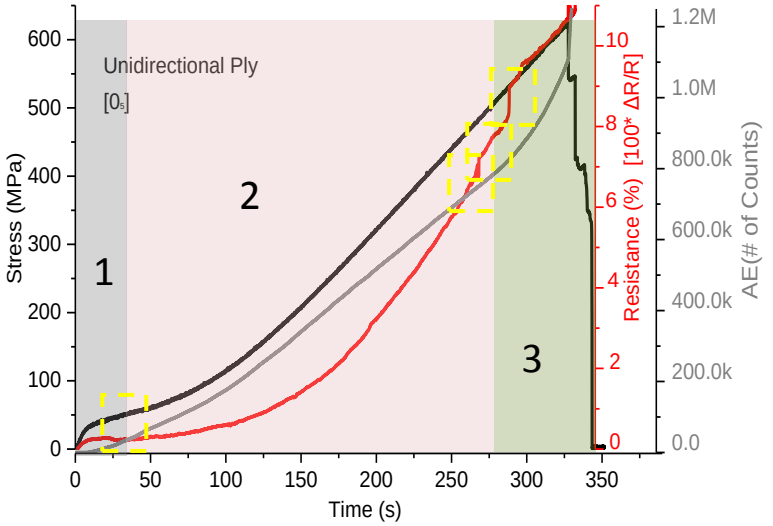
Unidirectional Ply
[0₅]
1
2
3
Stress (MPa)
Time (s)
Resistance (%) [100* ΔR/R]
AE(# of Counts)

b)

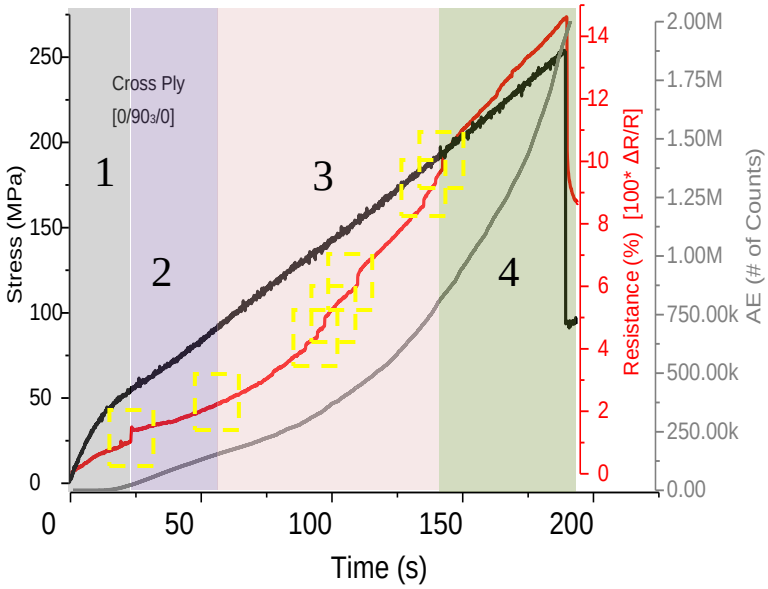
Cross Ply
[0/90₃/0]
1
2
3
4
Stress (MPa)
Time (s)
Resistance (%) [100* ΔR/R]
AE (# of Counts)

c)

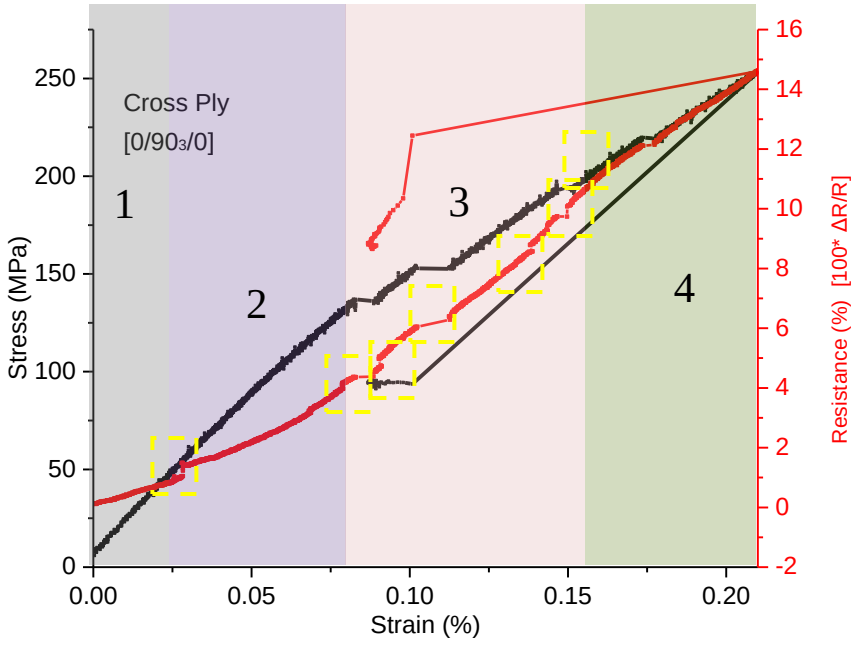

Figure 4.12 Graphs a, b, and c demonstrate the sensitivity of resistance (ΔR/R) to variations in resistance. Graph a) a unidirectional composite in tension, b) a cross ply composite in tension c) cross ply composite in tension with respect to time. Region 1; crack initiation, region 2; transverse microcracking, region 3; unidirectional strain, region 4; crack and delamination. Acoustic emissions in graphs confirm that damage in occurring in composites.

Unidirectional composites generally fail at a higher load than the cross-ply composites, due to the larger number of plies that carry the primary load. They failed at an average of 635 MPa while the cross-ply laminates failed at an average of 288 MPa. In Figure 4.12, failure is modeled using four stages of failure starting with crack initiation, transverse microcracking, unidirectional strain and finally cracking and delamination. Difference in each stage is determined by a change in the slope of the resistance curve or drastic increase in resistance. In both unidirectional and cross-ply

laminates, stage 1 exist before the composite has experience a stress of 50 MPa. During this stage, grows almost exponentially and the matrix of the composites begin to experience micro crack formation. In stage two, the load is transferred to the transverse plies and micro cracks coalesce in the 90-degree fibers. Transverse microcracking does not exist in unidirectional laminates due to the absence of 90 degree fibers. During transverse microcracking, which is characterized by the first change in the slope of the resistance, the 0 degree fibers in the cross ply laminates experience elastic but no permanent deformation. Once the transverse fibers in the cross ply laminates are unable to support the load, the load is then transferred to the 0 degree fibers. Stage 4, cracking and delamination, is characterized by an unusable resistance curves and massive jumps until the specimens fail as the resistance approaches infinity.

4.5 **Damage Progression**

Cyclic loading provides a method to examine the damage progression in unidirectional and transverse composites. Similar to the monotonic tests, the cyclic stressed composites also failed before reaching a 13% change of peak resistance as displayed in Figure 4.13. Unidirectional plies continue to fail at an average of 600 MPa and Transverse plies failed at an average of 266 MPa. Cyclic tests enable us to evaluate changes in elastic stiffness and permanent deformation incurred by the composite and compare with the changes in the baseline resistance. All specimens failed before researching a baseline resistance change of 6%. The first slope determines an area of elastic deformation and the second region indicates where permanent deformation begins.

a)

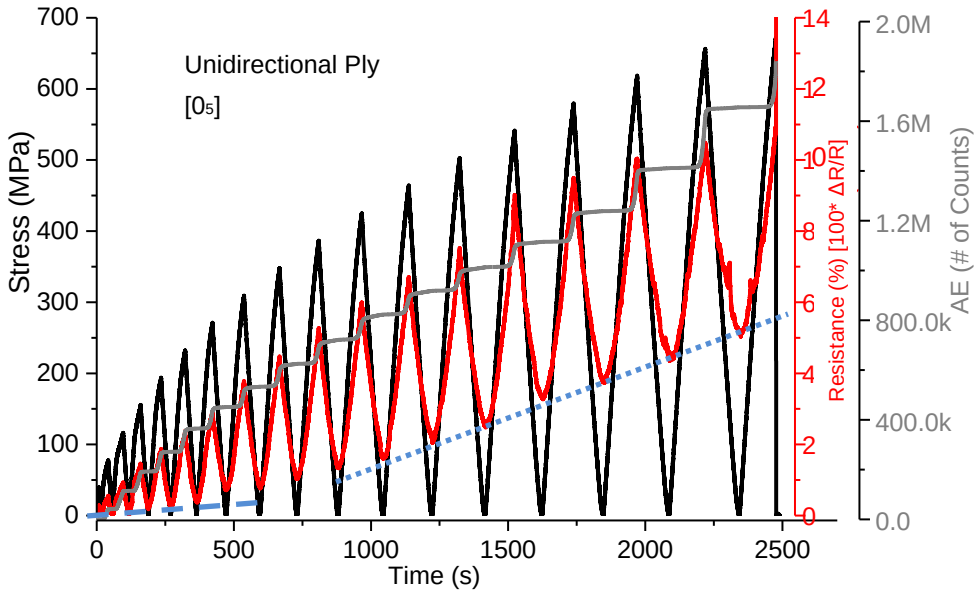
Unidirectional Ply
[0₅]
Stress (MPa)
Time (s)
Resistance (%) [100* ΔR/R]
AE (# of Counts)
0
100
200
300
400
500
600
700
0
500
1000
1500
2000
2500
0
2
4
6
8
10
12
14
0.0
400.0k
800.0k
1.2M
1.6M
2.0M

b)

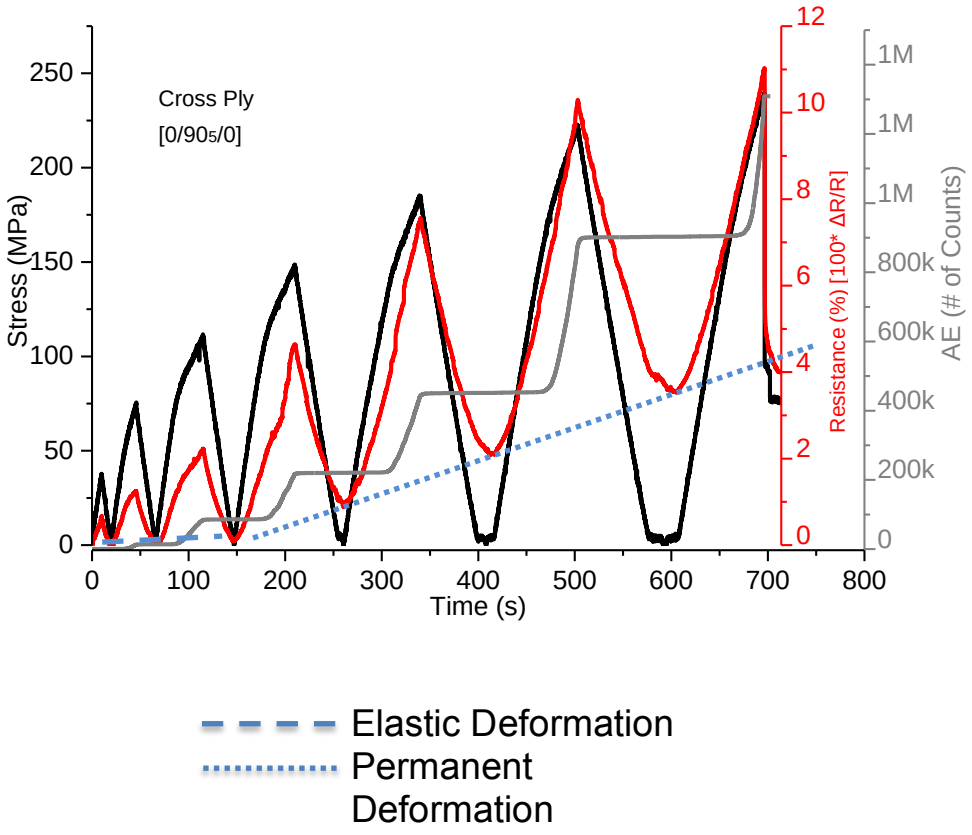

Figure 4.13 Acoustic emissions confirmed damage accumulation within the composite under cyclic loading conditions while the change in resistance exudes areas of deformation. First slope with dashed lines designated elastic deformation. Second slope with dotted lines designated permanent deformation. a.) Graph of unidirectional Laminates in cyclic loading conditions b.) Graph of Unidirectional Laminates in cyclic loading conditions

Unidirectional composites endured stress three times longer than transverse composites. Both orientations remain in the elastic region for the same amount of time reaching an average stress of 160 MPa and a baseline stress of 40 MPa. At the site where elastic deformation converted to permanent deformation, the slope of the

resistance curve changed by about 50%. Elastic deformation accounted for a third of the cycle. In real life applications, this region can be a great indicator that the device needs repair, since the material would not fail until the factor of safety reached 3. When plotted with respect to strain in Figure 4.14, carbon nanotube sensors distinguish the change in strain where permanent deformation occurs.

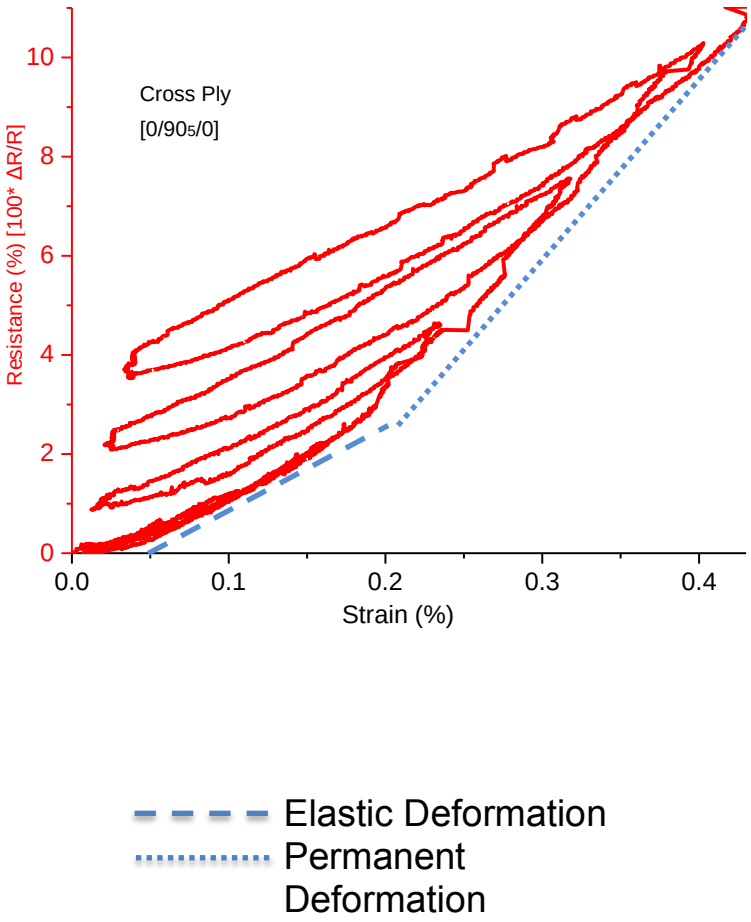

Figure 4.14 The graph displays cyclic loading conditions plotted with respect to strain. The dotted line indicates the differences in slope. The smaller slope designates elastic deformation and the stepper slope designates permanent deformation.

Under cyclic loading in Figure 4.15, nanotube sensors provide a description of the current state of damage of the composite. Sensors indicated a distinct area where the cracks in the composite begin to reopen, the existence of new damage, and the closing of cracks. The rate at which cracks reopened and closed displayed a similar linear relationship. The slope of the resistance curve indicated the cracks closed at the same pace that they opened. The region of new damage was confirmed by an increase in acoustic hits from a baseline slope of zero.

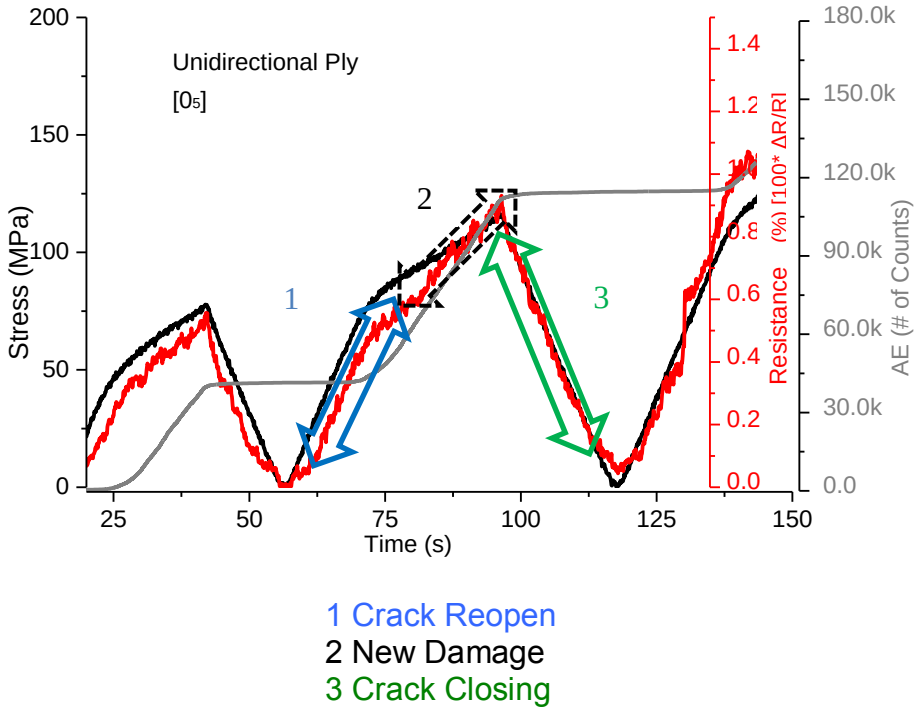

Figure 4.15 In a single cycle, section 1 represents crack reformation, section 2 represents the development of new damage, and section represents crack closure.

The area of new damage was also an indication of where new cracks formed and de-bonding of fibers was at its maximum. As the cycles progressed, the duration of new damage decreased but intensity increased, signaling that the composite was approaching failure. Once the region of cracks closing rose to a max of 13% and a max baseline of 6% fracture and delamination occurred.

4.6 **Damage Accumulation**

Each cycle provides information on how permanent changes in resistance correlates to deformation and crack accumulation. In Figure 4.16, Edge replication offers direct information on the formation of cracks in the composite and confirms the sensors' accuracy in reporting damage.

a)

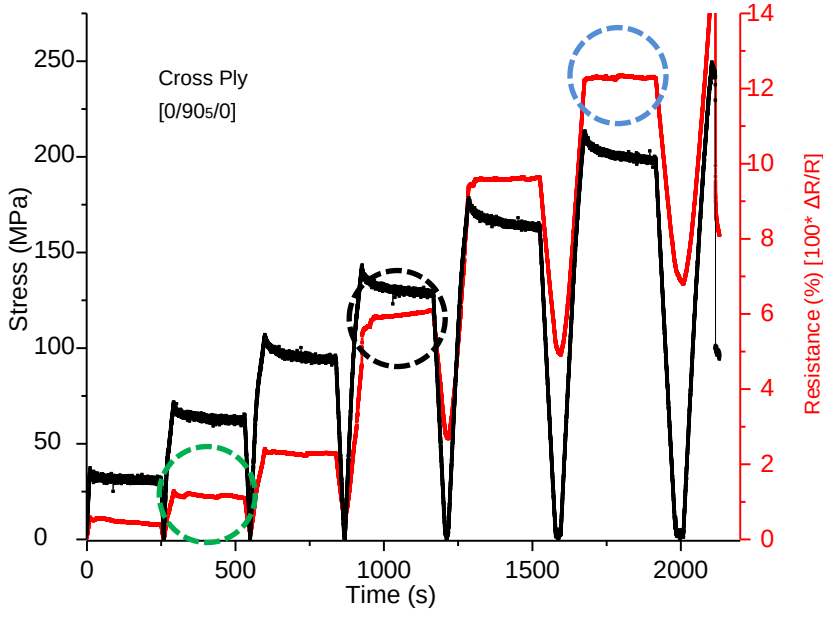

b)

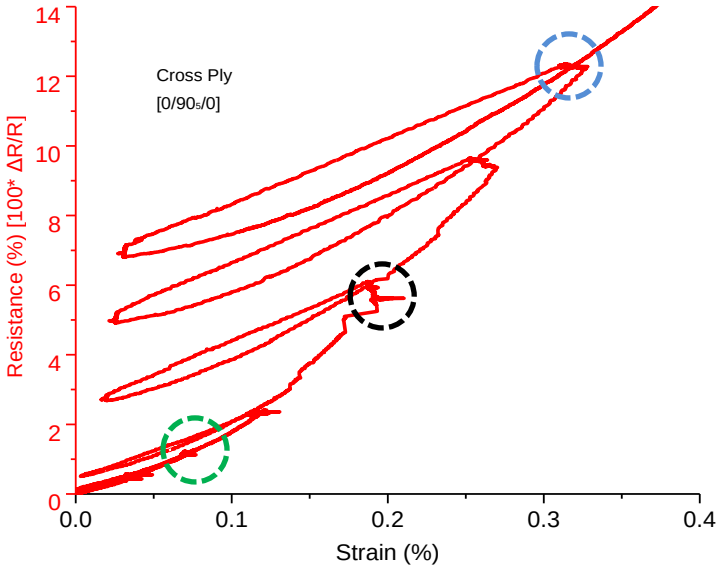

c)

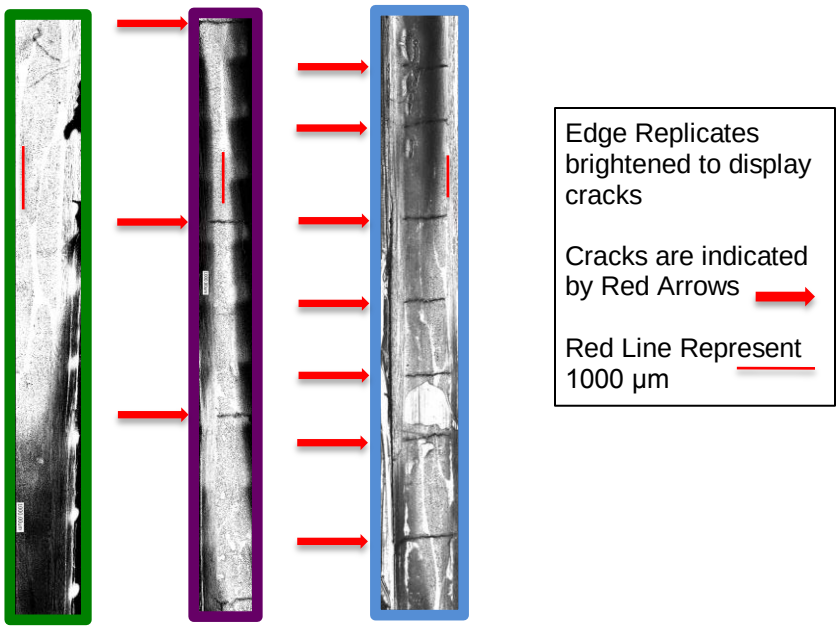

Figure 4.16 Edge replication provides confirmation of damage within composites. a) Cyclic loading with a hold time of 4 minutes loading, b.) Cyclic loading of cross ply laminates with respect to strain c.) Edge replicates of during cyclic loading.

In quasi-static tests, new damage and cracks are detected from spikes in the resistance curve or jumps in a linear slope. In cyclic loading, similar behavior is observed and is assumed to occur in the areas of new damage accumulation. As the material is under tensile stress, cracks fragment the percolating networks causing permanent deformation, which can be observed in the resistance curve.

Edge replicas were taken in areas where the resistance and stress curves had a slope of zero, held under constant load. In Figure 4.16, the second, fourth, and sixth displays the progression of cracks in the specimen. The second cycle was taken at a load of 70 MPa, a load of 125 MPa for the fourth cycle, and a load of 200MPa. Cracks were evenly spaced as they formed within the composite. The interval between the cracks decreased between each cycle, which confirmed permanent deformation, and the accumulation of damage within the composite.

4.7 **Graphene and Carbon Comparison to CNT**

Scholars have investigated other materials with potential damage sensing capabilities in composites. Graphene is a crystalline allotrope of carbon in the form of thin plates compared to carbon nanotubes cylindrical structure. In Figure 4.17, the resistance and strain results displays the usefulness of graphene as a sensor to analyze extension of the glass fibers in the composite.

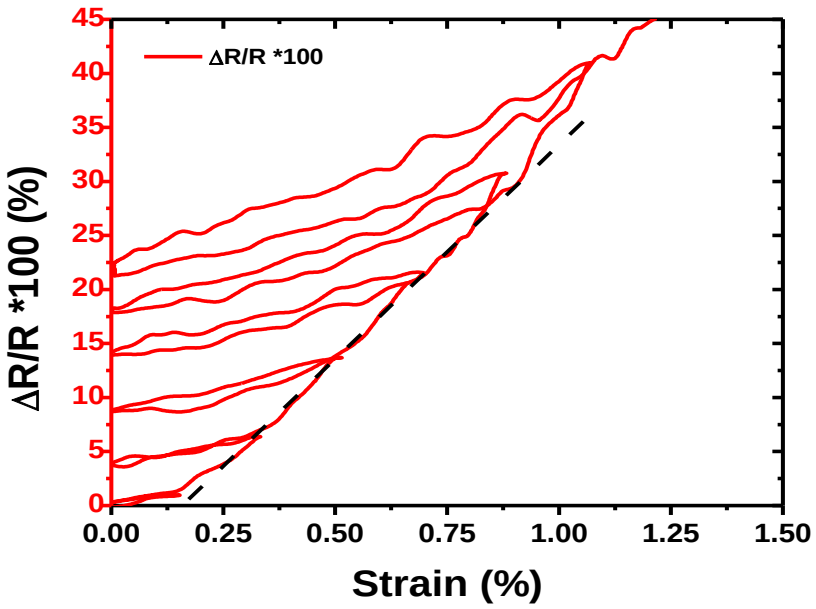

Figure 4.17 Graphene on E-glass fiber functions as a strain sensor.

Graphene fails to penetrate the matrix of the fibers preventing it from being reliable senor to analyze the micro scale nature of damage. The resistance immediately changes unlike the clear distinction between elastic and permanent deformation in CNT based sensor in Figure 4.14. Graphene electrical results contain noise and do not show clear jumps in resistance, which designates fiber breakage.

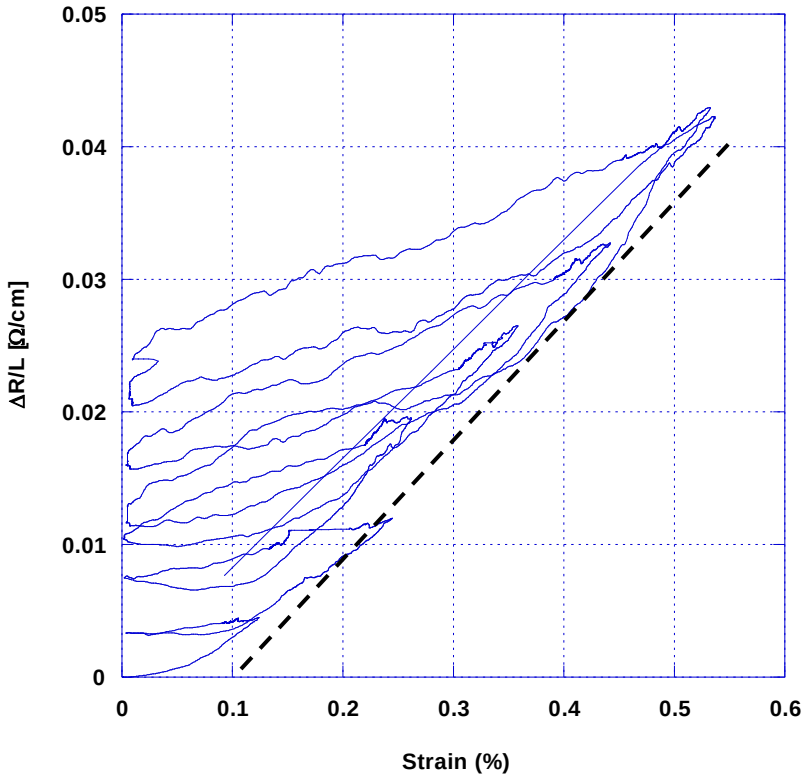

Figure 4.18 Carbon fiber composites function as a self strain sensor.

Carbon fibers remove the need for a conductive coating for a composite material. Carbon fiber reinforced polymer improves the strength and electrical properties, but is not able to sense micro damage and deformation like carbon nanotubes. Carbon fiber is not deposited into the interface of fibers so it can only sense damage within. Similar Graphene, it can be used as a strain sensor but not damage sensor. In Figure 4.18, the dotted line displays the linear behavior of the resistance curse. This means that the resistance does not display permanent and elastics deformation or show peaks in resistance to be correlated to fiber occurrences.

CNT provides the damage sensing capabilities to analyze fiber breakage, failure mechanisms, and predicting failure.

Chapter 5

CONCLUSION

5.1 Summary

Carbon nanotube ink sensors provide a new direction towards damage sensing applications in the analysis of strain and cracks in composite materials. The U-paddled mixer and three roll mill provided superior processing techniques to create tailorable inks that impeded wicking and enabled a complete dispersion of CNT into the ink. The addition of cellulose, Polyox and PVP enhanced the rheology of the ink and offered a stable solution for patterned printing. One weight percentage or each of the chemicals milled with one weight percent of nanotubes formed a percolating conductive network of nanotubes to be used as piezoresistive sensors. The resistance change of the inks hold potential for monitoring the structural health of composites.

Acoustic emission and edge replications confirmed the accuracy of the resistance measurements to evaluate the amount of stress and strain in the composite. During quasi-static tests, resistance curves indicated four regions of damage that determined the current mode of failure experience by the composite. In region one, crack initiation, micro cracks began to form in the polymer enclosing the matrix of the fabric fragmented resulting in material failure. Transverse micro cracking occurred in the second region. In cross ply laminates, the fibers began to separate until the cracks reached the interface of the 0° fibers. In the third region the loads were transferred to the 0° fibers ending the phase of elastic deformation and converting to permanent deformation. As stress increased, an increase in resistance and spikes designated areas

of de-bonding in individual fibers. The last region, fracture and delamination, displayed a region of instability in the composite. The jumps and an increase to infinite resistance indicated material failure.

Cyclic tests provided an advanced examination of deformation in the composite. The sensors specified two areas where the behavior of the material began to change. Once the slope of the baseline resistance reached 6%, failure was initiated in the composite. The first slope determined elastic deformation followed by a 50% increase indicating permanent deformation. Three regions in the each cycled displayed the conditions of crack formation. Each cycle followed a trend where the resistance increased to show cracking reopening followed by an adjustment in slope showing new damage. The decrease of the slope at the same rate it resistance increased in the last region illustrated crack closing. Edge replicas confirmed the formation of new damage in the composite.

The ability to monitor damage progression and accumulation in composites verifies carbon nanotube ink as a viable candidate for piezoresistive sensors. Changes in resistance provide an understanding of the modes of failure and an accurate prediction of when composites will fail. The commercialization of composites and taken over industries with products around the globe. Aircraft, cars, and devices are among the top outcomes of composite materials. The need for development of monitoring systems is high in these goods. Nanotube ink sensors provide a feasible solution for the need of damage screening devices.

5.2 **Path forward**

5.2.1 Advanced Characterization Techniques

The development of nanotube ink sensors calls for many processing techniques and methods to achieve desired rheology and print quality. In this research, rheology was analyzed through qualitative viscosity measurements and print quality through contrast examinations and the deviation of the inks. These measurements provide preliminary knowledge on the behavior of the inks but do not provide enough information regarding the orientation of fibers and dispersions of CNT. Pandey and Thostenson [10] discussed the use of transmission electron microscopy (TEM) and scanning electron microscopy to analyze dispersions of CNT and the characteristics of single fibers with polymers. Similar test can be done to analyze dispersions of CNT into the ink precursors. Higher resolution images will produce further knowledge effects of agglomerates in the solutions and give an advance examination of the polymer and ink filled matrix of the fabric. The knowledge can be used to further enhance the performance of the CNT inks ability to monitor damage progression.

5.2.2 Ink Jet Printing

Pattern printing using the screen-printing technique allows accuracy in the millimeter range supplying a synopsis of damage accumulation in the entire composite.

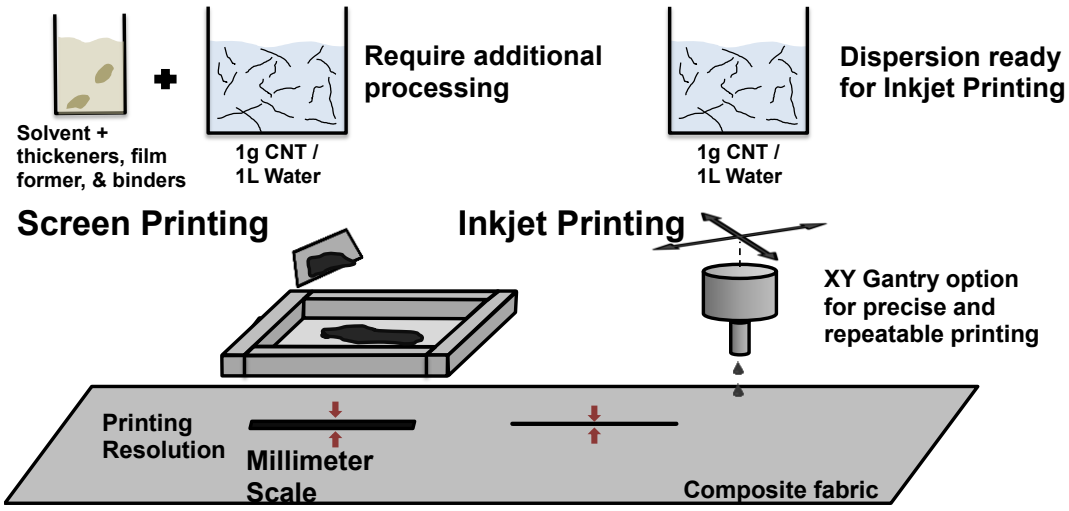

Figure 5.1 Inkjet printing (right) provides a more precise ink depositon than screen printing (left).

To understand the development of cracks and failure in a prescribed area or individual fibers, a more precise deposition is required. Kroger *et al.* [8] and Sanchez *et al.* [13] used to DEK ink jet printers for the fabrication of biosensors and immunosensors. Similar techniques can improve the ability to detect cracks and depict the model for material failure to higher levels. Ink jet printing allows specific sites on interest to be studied instead of probing a general area. Application of such techniques will eliminate the need of acoustic emission and edge replication to confirm strain and crack occurrence.

5.2.3 Live Models and Computational Analysis

The next step in this research should explore the effects of the localized sensors placed in discrete areas on the composite. Increasing the number of sensors provides understanding of the failure mechanisms enclosing the site of interest. When

the material is under simultaneous loading conditions and various types failure mechanisms, multiple sensors is required to analyze damage and trace crack propagation in composites. Interpreting electrical responses from numerous sensors allow multi-dimensional representation of material failure to be generated. Further computational analysis and data reduction will summarize the damage progression and accumulation of cracks within campsites.

REFERENCES

[1] Adsul, Mukund G., Digambar V. Gokhale, and Diego A. Rey. "Combined Strategy for the dispersion/dissolution of Single Walled Carbon Nanotubes and Cellulose in Water." *Journal of Materials Chemistry.* 21.7: 2054-2056. (2011).

[2] Choi, Nak-Sam, Tae-Won Kim, and Kyoung Y. Rhee. "Kaiser Effects in Acoustic Emission from Composites during Thermal Cyclic-Loading." *NDT & E International.* 38.4: 268-274. (2005).

[3] Gao, Limin, Erik T. Thostenson, Zuoguang Zhang, and Tsu-Wei Chou. "Sensing of Damage Mechanisms in Fiber-Reinforced Composites Under Cyclic Loading using Carbon Nanotubes." *Advanced functional materials*. 19.1: 123. (2009).

[4] Gao, Limin, Erik T. Thostenson, Zuoguang Zhang, and Tsu-Wei Chou. "A Comparative Study of Damage Sensing in Fiber Composites using Uniformly and Non-Uniformly Dispersed Carbon Nanotubes." *Carbon.* 48.13: 3788-3794. (2010).

[5] Gao, Limin, Erik T. Thostenson, Zuoguang Zhang, and Tsu-Wei Chou. "Coupled Carbon Nanotube Network and Acoustic Emission Monitoring for Sensing of Damage Development in Composites." *Carbon.* 47.5:1381-1388. (2009).

[6] Gyuhae, Park, Charles R. Farrar, Francesco Lanza di Scalea, and Stefano Coccia. "Performance Assessment and Validation of Piezoelectric Active-Sensors in Structural Health Monitoring." *Smart Materials and Structures*.15.6: 1673. (2006).

[7] Jung, Yong Chae, et al. "Transparent and Conductive Polyethylene Oxide Film by the Introduction of Individualized Single-Walled Carbon Nanotubes." *Macromolecular Rapid Communications.* 30.24: 2084-2048. (2009).

[8] Kröger, Silke, and Anthony P. F. Turner. "Solvent-Resistant Carbon Electrodes Screen Printed Onto Plastic for use in Biosensors." *Analytica Chimica Acta*. 347.1–2: 9-18. (1997).

[9] Lain-Jong, Li, Chien-Yen Chen, R. C. Darton, R. J. Nicholas, and S.C.Baker. "Comparative Study of Photoluminescence of Single-Walled Carbon Nanotubes Wrapped with Sodium Dodecyl Sulfate, Surfactin and Polyvinylpyrrolidone." *Nanotechnology*. 16.5: S202. (2005).

[10] Pandey G., Erik T. Thostenson. "Carbon Nanotube-Based Multifunctional Polymer Nanocomposites." *Polymer Reviews.* 52.3-4: 355-416. (2012).

[11] Pu, Hong Ting, et al. "Effects of Polyvinylpyrrolidone and Carbon Nanotubes on Magnetorheological Properties of Iron-Based Magnetorheological Fluids." *Journal of Applied Polymer Science.* 102.2: 1653-7. (2006).

[12] Rafiee, Banafsheh, and Ali Reza Fakhari. "Electrocatalytic Oxidation and Determination of Insulin at Nickel Oxide Nanoparticles-Multiwalled Carbon Nanotube Modified Screen Printed Electrode." *Biosensors and Bioelectronics.* 46:130-5. (2013).

[13] Sánchez, Samuel, Martin Pumera, and Esteve Fàbregas. "Carbon nanotube/polysulfone Screen-Printed Electrochemical Immunosensor." *Biosensors and Bioelectronics.* 23.3: 332-340. (2007).

[14] Shi, Yong Sheng, et al. "Large Area Screen-Printing Cathode of CNT for FED." *Diamond and Related Materials*. 12.9: 1449-52. (2003).

[15] Thostenson, Erik T., and Tsu-Wei Chou. "Real-Time in Situ Sensing of Damage Evolution in Advanced Fiber Composites using Carbon Nanotube Networks." *Nanotechnology*. 19.21. (2008).

[16] Thostenson, Erik T., and Tsu-Wei Chou. "Carbon Nanotube Networks: Sensing of Distributed Strain and Damage for Life Prediction and Self Healing." *Advanced Materials*. 18.21: 2837-2841. (2006).

[17] Wan, Jun, et al. "A Simple Method for Preparing Biocompatible Composite of Cellulose and Carbon Nanotubes for the Cell Sensor." *Sensors and Actuators B: Chemical.*146.1: 221-225. (2010).

[18] Yukui, Li, Zhu Changchun, and Liu Xinghui. "Field Emission Display with Carbon Nanotubes Cathode: Prepared by a Screen-Printing Process." *Diamond and Related Materials*.11.11: 1845-1847. (2002).

Appendix A Images of Specimen During Manufacturing

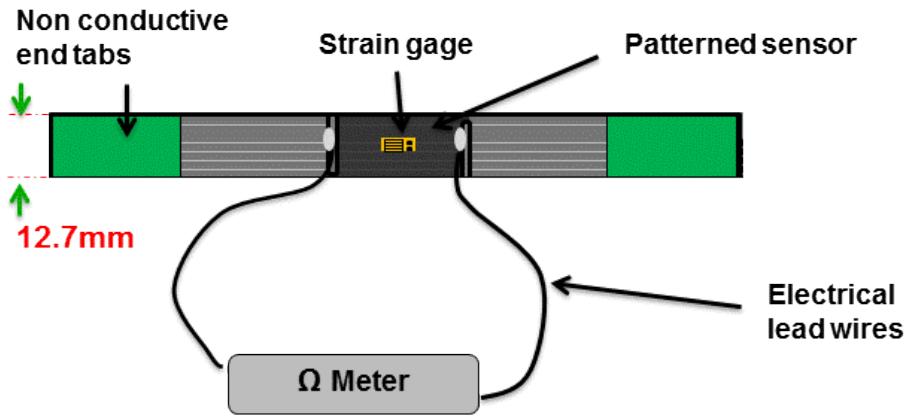

Figure A.1 Diagram of top view of CNT sensor

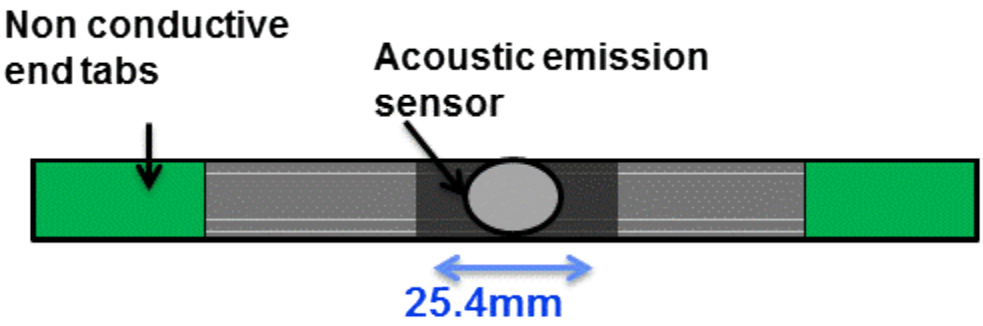

Figure A.2 Diagram of front bottom view of CNT sensor

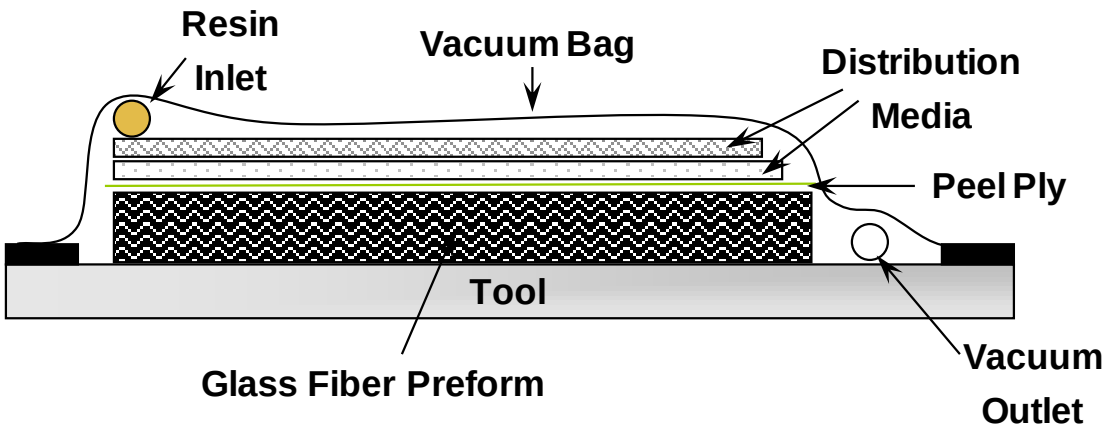

Figure A.4 Diagram of VARTM Setup

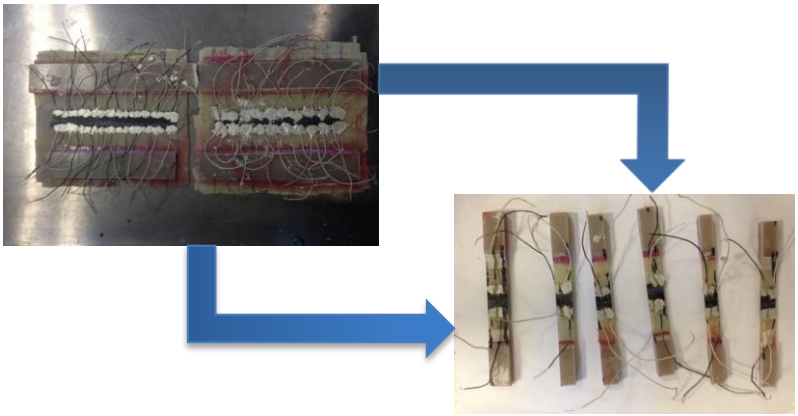

Figure A.4 Diagram of top view of CNT sensor after VARTM and Sliced

Appendix B Tables of Ink Characterization

Table B.1 Non-Carbon Nanotube Based Solutions

Name	CNT Base	% Base	Solvent added	% Solvent	% Cellulose	% Polyox	% PVP	Processing
RB1	None	100	TRD Water	97	1	1	1	Thinky
RB2	None	100	TRD Water	98.5	0.5	0.5	0.5	Thinky
RB3	None	100	TRD Water	98	0.5	0.5	1	Thinky
RB4	None	100	TRD Water	98	0.5	1	0.5	Thinky

Table B.2 Carbon Nanotube Based Solutions

Name	CNT Base	% Base	Solvent added	% Solvent	% Cellulose	% Polyox	% PVP	Processing
AA	Ozone CNT	100	None	97	1	1	1	Thinky
AB	Ozone CNT	100	None	98.5	0.5	0.5	0.5	Thinky
AC	PEI CNT	100	None	97	1	1	1	Thinky
AD	PEI CNT	100	None	98.5	0.5	0.5	0.5	Thinky
AE	Ozone CNT	100	None	98	0.5	1	0.5	Thinky
AF	Ozone CNT	100	None	97.5	1	1	0.5	Thinky
AG	Ozone/PEI CNT	50/50	None	97	1	1	1	Thinky
AH	Ozone CNT	100	None	92	1	2	5	Thinky
AI	Ozone CNT	100	None	93	1	1	5	Thinky
AJ	Ozone CNT	100	None	93	2	0	5	Thinky

Table B.3 Water Based Ideal Solutions

Name	CNT Base	% Base	Solvent added	% Solvent	% Cellulose	% Polyox	% PVP	Processing
0.5111	Water/0.5% CNT	100	TRD water	97	1	1	1	Mixer/3 roll/Thinky
1111	Water/1% CNT	100	TRD water	97	1	1	1	Mixer/3 roll/Thinky
2111	Water/2% CNT	100	TRD water	97	1	1	1	Mixer/3 roll/Thinky

Table B.4 Additive Characterization

INK	Surface Tension (Degrees)					
	Trial 1	Trial 2	Trial 3	Trial 4	Trial 5	AVG
Water	46.514	22.491	37.643	32.477		34.78125
Cell.1	56.943	48.186	53.977	53.317	56.787	53.842
Cell.2	58.431	59.796	57.323	56.806	32.302	52.9316
α2	28.57	35.891	33.827	25.088	33.456	31.3664
γ	20.619	21.753	22.563	20.401		21.334
δ	31.577	32.061	27.71	53.94	52.02	39.4616
ε	55.745	59.401	59.893	64.875		59.9785
ζ	42.946	41.366	41.679	32.305		39.574
η	46.806	55.511	51.986	51.832	53.702	51.9674
θ	55.659	56.316	56.6009	56.06		56.158975